Supporting Information

A water-soluble Pd_4 molecular tweezer for selective encapsulation of isomeric quinones and their recyclable extraction

Dharmraj Prajapati[a], Pallab Bhandari[a], Ennio Zangrando[b] and Partha Sarathi Mukherjee[a]*

[a]*Department of Inorganic and Physical Chemistry, Indian Institute of Science, Bangalore-560012, India* Email: psm@iisc.ac.in

[b]*Department of Chemical and Pharmaceutical Sciences, University of Trieste, Trieste 34127, Italy.*

Materials and methods:

All the chemicals and solvents were purchased from different commercially available suppliers and directly used without further purification. NMR studies were performed on Bruker 400 and 500 MHz spectrometers. The chemical shifts (δ) are accounted in parts per million (ppm) unit relative to tetramethylsilane (Me_4Si) as an internal standard (0.0 ppm), and proton resonance appeared due to incomplete deuteration of the solvents $CDCl_3$ (7.26 ppm), $(CD_3)_2SO$ (2.50 ppm) and D_2O (4.79 ppm). ^{13}C NMR spectra were collected on the same instruments at 100 MHz, 125 MHz, and chemical shift (δ) were assigned in ppm units relative to external $CDCl_3$ at 77.4-76.8 ppm. Electrospray ionization mass spectrometry (ESI-MS) experiments were recorded on an Agilent 6538 Q-TOF ESI-MS instrument using spectroscopic grade solvents. All the UV-Vis studies were carried out on a PerkinElmer Lambda-750 spectrophotometer.

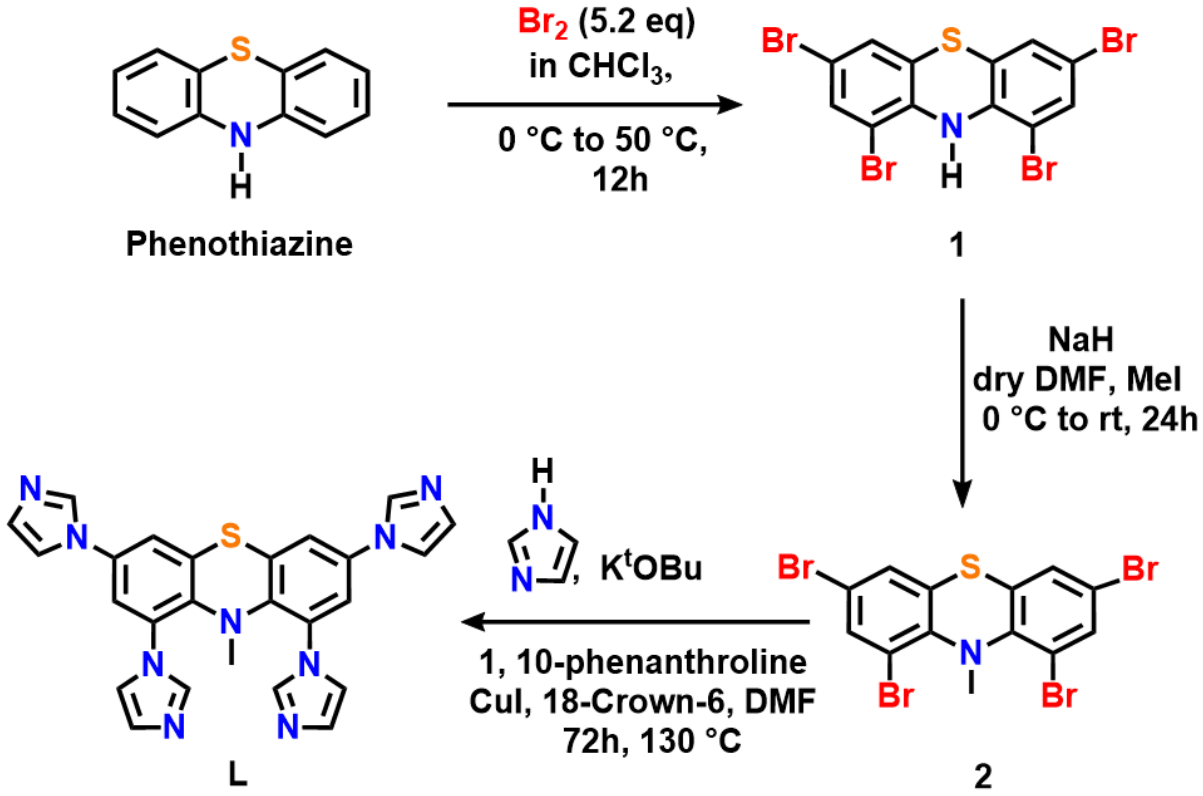

Scheme S1: Synthetic route of ligand **L**.

Synthesis of 1,3,7,9-tetrabromo-10*H*-phenothiazine (1):

Compound **1** was synthesized by bromination of phenothiazine in 89% yield according to the literature procedure.[1] In a 100 mL round-bottom flask, phenothiazine (1 g, 5.02 mmol) was dissolved in 25 mL chloroform and into that Br_2 (5.2 eq) diluted in chloroform (5 mL) was added dropwise at room temperature. The resulting reaction mixture was stirred at 50 °C for 12 h. After completion of the reaction, the reaction was quenched with hydrazine at 0 °C and methanol was added. The precipitates were filtered and washed with MeOH, H_2O, MeOH and hexane to isolate 1,3,7,9-tetrabromo-10*H*-phenothiazine (**1**) (2.23 g, 89 %) as a grey solid. ^{1}H NMR (400 MHz, $CDCl_3$): δ 7.39 (d, 2H, *J* = 2.04 Hz), 7.14 (brs, 1H), 7.03 (d, 2H *J* = 1.96 Hz),). ^{13}C NMR (125 MHz, $CDCl_3$): δ 137.72, 133.16, 128.15, 121.07, 114.90, 110.42.

Synthesis of 1,3,7,9-tetrabromo-10-methyl-10*H*-phenothiazine (2):

A 100 mL oven-dried Schlenk flask was charged with 1,3,7,9-tetrabromo-10*H*-phenothiazine (1000 mg, 1.94 mmol) and 20 mL dry DMF. Solid NaH (60 % in paraffin oil, 155.2 mg, 3.88 mmol) was added very slowly at 0 °C temperature. The resulting slurry was stirred for 1 h at

room temperature. Iodomethane (550.7 mg, 3.88 mmol) was added to the above mixture and kept for stirring for 24 h until the completion of the reaction was indicated by TLC. The final reaction mixture was poured into 200 mL water to get precipitate which was collected by filtration and dried under vacuum. Isolated yield: 57 % (583.7 mg, 1.11 mmol). ^{1}H NMR (400 MHz, $CDCl_3$): δ 7.62 (d, 2H), 7.30 (d, 2H), 3.23 (s, 3H).

Synthesis of L:

An oven-dried 100 mL two-necked round bottom flask was degassed and charged with CuI (93.32 mg, 0.49 mmol), 1,10-phenanthroline (176.4 mg, 0.98 mmol) and dry DMF (5 mL). The brown solution was heated at 110 °C for 5 min. **2** (1300 mg, 2.46 mmol), imidazole (2676.9 mg, 39.32 mmol), potassium tert-butoxide (4830.64 mg, 43.05 mmol) and a pinch of 18-crown-6 were added to the above solution and the final mixture was heated at 130 °C for 72 h. The final brown residue was stirred with 100 mL of water for 10 min and then filtered. The residue washed thoroughly with water and then dried. The residue was extracted with 200 mL methanol followed by treatment with sodium sulphate. Evaporation of the solvent yielded dirty white solid which was recrystallized from methanol/water solvent mixture to get pure L as a crystalline material **L**. Isolated yield: 563.89 mg (48%). ^{1}H NMR (400 MHz, CDCl3): δ =7.83 (s, 2H), 7.61(s, 2H), 7.30(d, 2H), 7.24(br, 6H), 7.15(d, 2H), 7.03(s, 2H), 2.50(s, 3H). ^{13}C NMR (100 MHz, CDCl3): δ = 140.34, 137.42, 135.35, 134.82, 134.09, 131.89, 131.32, 130.77, 120.52, 120.18, 119.50, 117.92, 43. ESI MS: m/z calcd for $[L+H]^+$ = 478.1562 (found 478.1480), $[L+ Na]^+$ = 500.1382 (found 500.1311).

Synthesis of Pd_4L_2 molecular tweezer (MT):

The solid tetraimidazole ligand **L** (50 mg, 0.105 mmol) was dissolved in 3 mL DMSO and the clear solution was added to another 2 mL DMSO solution of cis-(tmeda) $Pd(NO3)_2$ **M**(72.59 mg, 0.21 mmol) and the clear solution was heated at 60 °C for 12 h. The light-yellow solution was then allowed to reach room temperature and was treated with 100 mL ethyl acetate to obtain white precipitate which was collected by centrifugation followed by washing with excess of ethyl acetate. Isolated yield: 122 mg (96 %). ^{1}H NMR (400 MHz, D_2O): δ 8.74 (s, 2H), 8.68 (s, 2H), 8.41 (d, 4H), 6.70 (s, 2H), 7.67 (s, 2H), 7.64 (s, 4H), 7.62 (s, 4H) 7.56 (s, 2H), 7.54 (s, 2H), 7.52 (s, 2H), 7.50(s, 2H), 7.44(d, 4H) 3.13-3.08(br, 16H), 2.98-2.86(d, 12H), 280-2.77(m, 12H), 2.75-2.720(m, 24H), 2.38(s, 3H), 2.29(s, 3H). ESI-MS: (CH_3CN): m/z 1358.1048 $[M_4L_2(PF_6)_6]^{2+}$ (calcd 1358.1222), 857.4022 $[M_4L_2(PF_6)_5]^{3+}$ (calcd 857.4292), 607.0587 $[M_4L_2(PF_6)_4]^{4+}$ (calcd 607.0826), 455.56 $[M_4L_2(6PF_6)_3]^{5+}$ (calcd 455.8675).

General guest gncapsulation procedure: A 0.5 mL D_2O solution of **MT** (5 mg, 0.0021 mmol) was stirred for 12 hours with five equivalents of each solid quinone guests respectively at room temperature and centrifuged to remove unencapsulated excess guest. The resulting clear supernatant was examined by NMR.

Selective extraction of PQ (Phenanthrenequinone) from AQ (Anthraquinone):

To a 1mL H_2O (5 mg, 0.0021 mmol) colourless solution of **MT** in a 4 mL glass vial, 3 mg (0.014 mmol) of each **PQ** and **AQ** were added. The resulting suspension was stirred for 12 hours at room temperature and centrifuged to remove unencapsulated excess guest. The supernatant containing host-guest complex was treated with $CDCl_3$ to extract guest molecules. ^{1}H NMR experiment was carried out to calculate the composition of the $CDCl_3$ extract using 1,3,5-trimethoxybenzene as an internal standard. The aqueous solution after extraction of the guest was reused for five cycles. To check the efficiency of extraction from a practical perspective, equimolar mixture of **PQ** and **AQ** was added to D_2O solution of **MT** and ^{1}H NMR of the mixture was monitored with time. Complete extraction of **PQ** from **AQ** was observed after 4 hours stirring at room temperature.

UV-Vis studies for guest encapsulation: A stock aqueous solution of 10^{-3} M (0.5 mL) of each host-guest complex was achieved by encapsulating respective guest at room temperature for 12 h. A 10^{-5} M (2 ml) H_2O sample was prepared by adding required amount of the stock solution and UV-vis spectrum was recorded at room temperature.

Single crystal data collection and structure solution of MT:

Diffraction data of a single crystal of compound **1** were collected at the X-ray diffraction beamline (XRD1) of the Elettra Synchrotron of Trieste (Italy), with a Pilatus 2M image plate detector. The dataset was collected at 100 K with a monochromatic wavelength of 0.700 Å, through the rotating crystal method. The diffraction data were indexed, integrated and scaled using XDS[2]. The structure was solved by direct methods using SIR2014[3] and subsequent Fourier analysis and refinement with the full-matrix least-squares method based on F^2 were performed with SHELXL[4]. The intensity data were treated with program Squeeze (of Platon Package)[5], which revealed a small potential solvent area volume of 1022.6 Å^3, correspondent to 8.7% of the unit cell. Hydrogen atoms were placed at calculated positions except those of disordered 15 water molecules. Due to the disorder observed in the crystal, a total of 14 nitrate anions and 3 acetone molecules were detected in the Fourier map. Refinements were performed with restrains on bond distances and thermal factors.

Crystal data: $C_{157}H_{222}N_{66}O_{60.5}Pd_8S_4$, M = 4981.43, triclinic, space group *P* $\bar{1}$, *a* = 18.719(4), *b* = 21.435(4), *c* = 30.531(6) Å, α= 72.94(3), β = 89.08(3), γ = 88.27(3)°, *V* = 11705(4) $Å^3$, Z = 2, ρ_{calcd} = 1.413 g/cm^3, μ(Mo-Kα) = 0.620 mm^{-1}, *F*(000) = 5084. Final *R* = 0.0571, *wR2* = 0.1750, *S* = 1.025 for 2884 parameters and 255979 reflections, 64791 unique [R(int) = 0.0199], of which 58961 with I > 2σ(I), max positive and negative peaks in difference Fourier map = 2.460 and -2.275 e. $Å^{-3}$. **Deposition number**: CCDC 2259512.

The asymmetric unit comprises two comparable cationic tetranuclear complexes of formula $[C_{74}H_{102}N_{26}Pd_4S_2]^{2+}$, counterbalanced by nitrate anions, beside some acetone and water molecules.

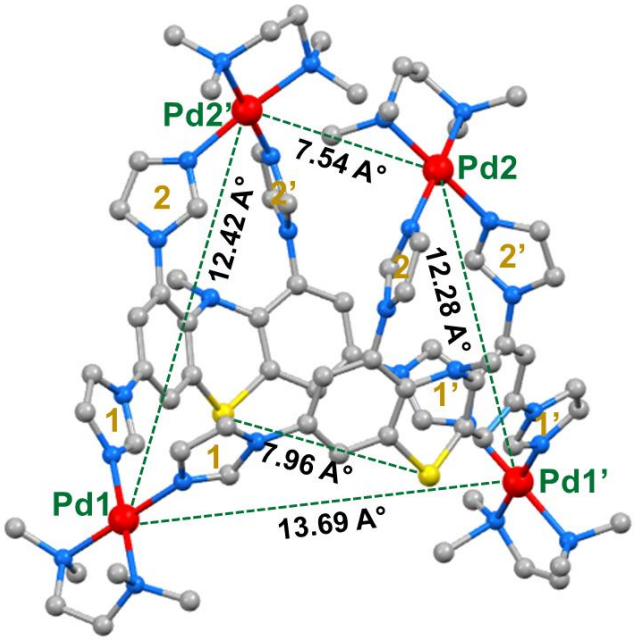

Fig. S1 Molecular structure (ball stick model) of one of the two independent complexes that exhibit a pseudo C_{2v} symmetry (no H atoms displayed for clarity) Color code: C = grey, N = Blue, S = yellow, and red = Pd.

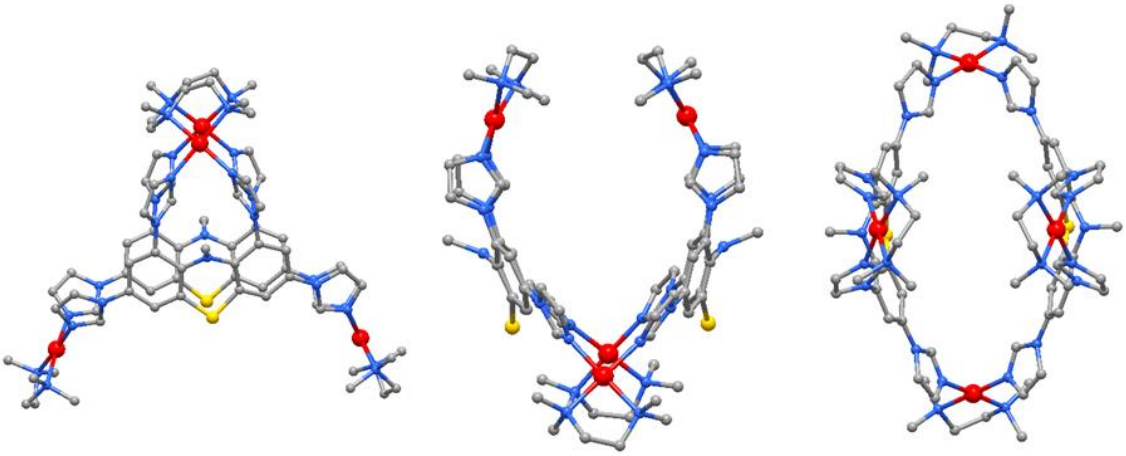

Fig. S2 Three perspective views of the tetranuclear complex MT. (no H atoms displayed for clarity) Color code: C = grey, N = Blue, S = yellow, and red = Pd.

Computational studies: Full geometry optimizations of the host (**MT**) and all the host-guest complexes were carried out by a PM6 semi-empirical method using the Gaussian 16 package.[6] In all the calculations, solvation was introduced using the Polarization Continuum model (PCM), choosing water as a solvent for better comparison with the experimental results. First, the geometry of the free host (**MT**) was optimized. Subsequently, geometry optimization for all the host-guest inclusion complexes was carried out by freezing computationally obtained coordinates of the host (**MT**) molecule. Finally, single point energies for all the optimized host-guest structures were calculated using the hybrid B3LYP functional with a mixed basis set of LanL2DZ (for Pd atom) and 6-31g (for C, H, N, S and O atoms).

Table S1. Calculated single point energies from DFT method

Host-guest complexes	**Energy (a.u.)**	**Energy (Kj/mol)** [1 a.u. = 2625.5 Kj/mol]
AQ⊂MT	-9254.52099450	-24297744.87
PQ⊂MT Diketone groups oriented downward **(towards Pd1, Pd1')**	-9255.58777408	-24300545.70
PQ⊂MT Diketone groups oriented upward **(towards Pd2, Pd2')**	-9260.58466126	-24313665.03

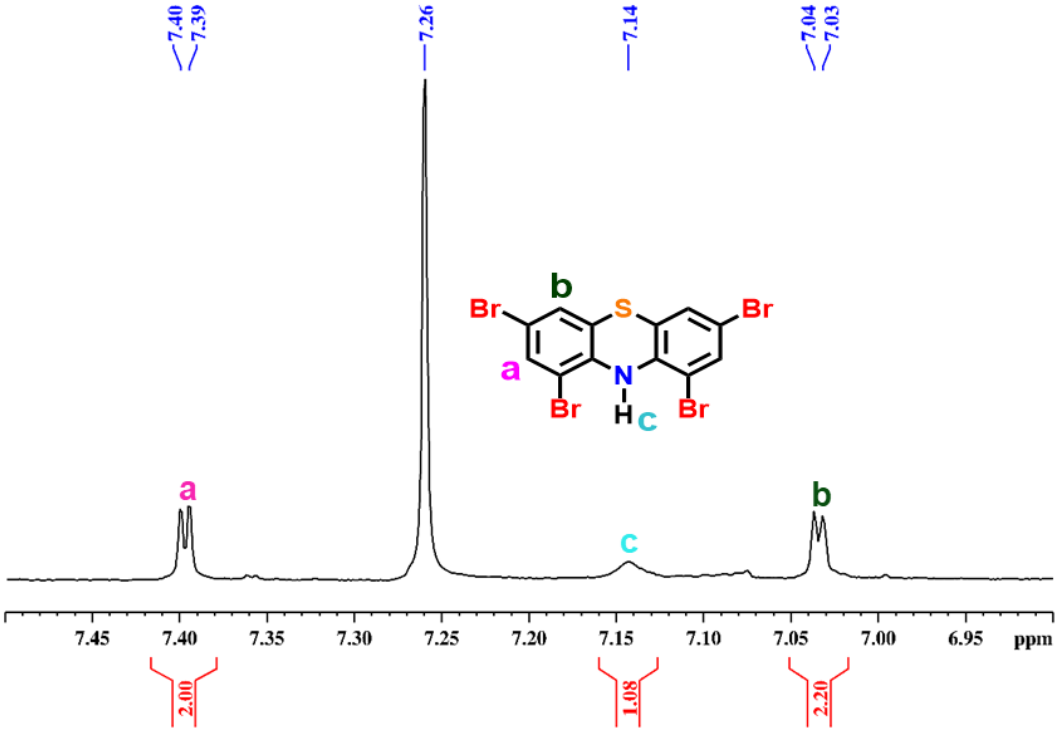

Fig. S3 ^{1}H NMR spectrum of **1** recorded in $CDCl_3$.

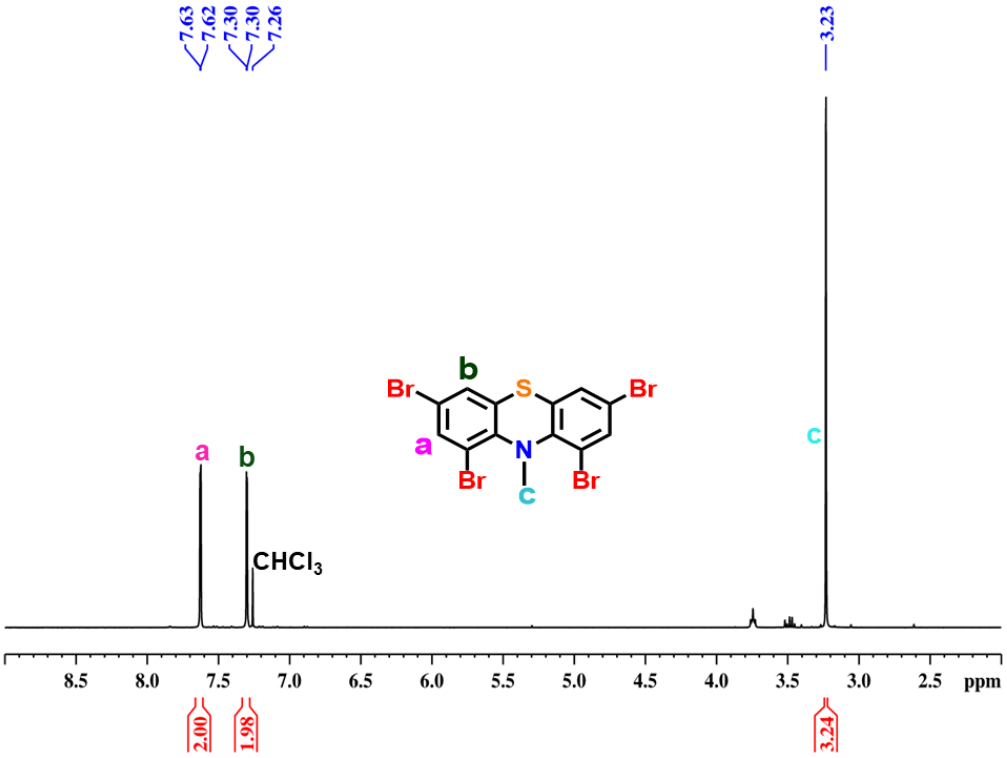

Fig. S4 ^{1}H NMR spectrum of **2** recorded in $CDCl_3$.

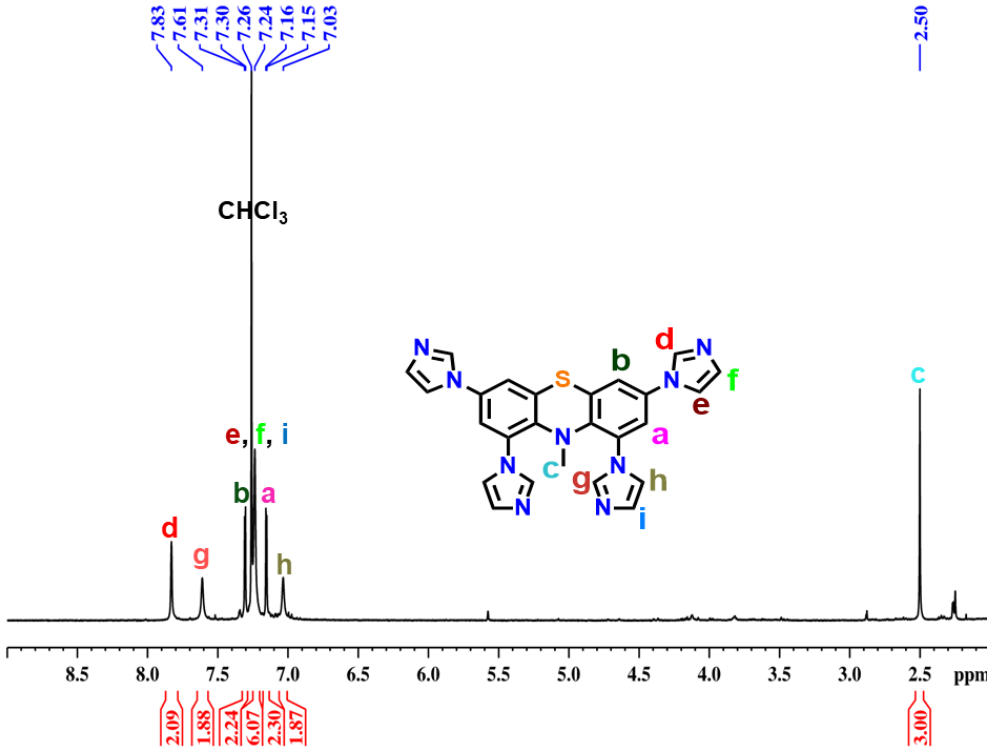

Fig. S5 ^{1}H NMR spectrum of **L** recorded in $CDCl_3$.

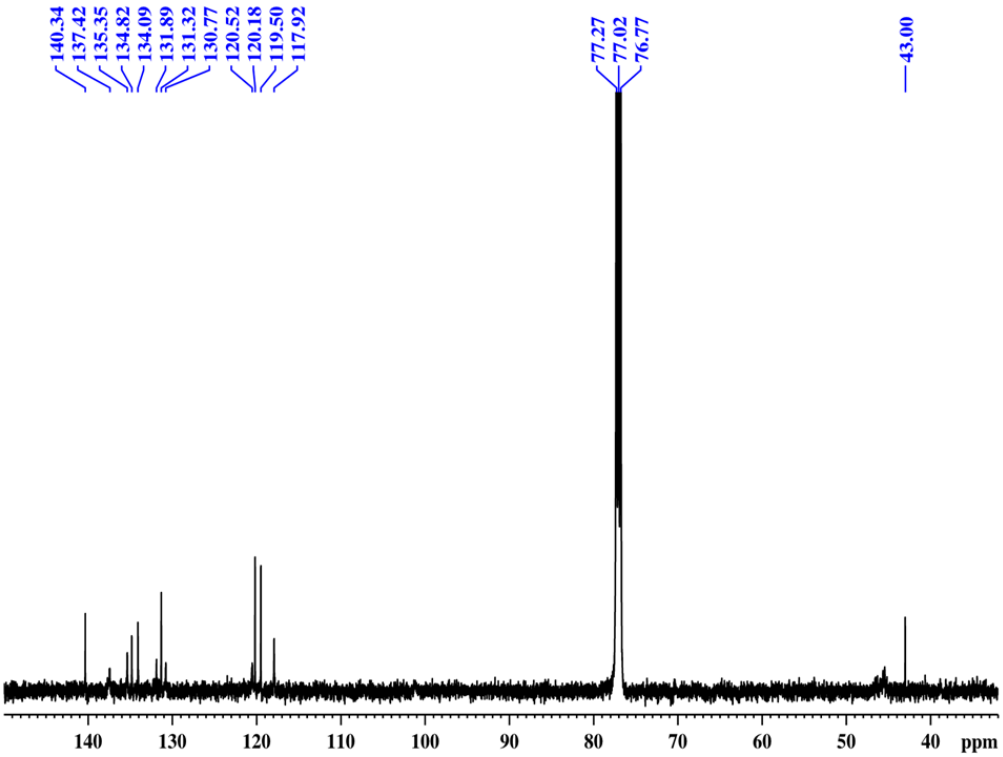

Fig. S6 ^{13}C NMR spectrum of **L** recorded in $CDCl_3$.

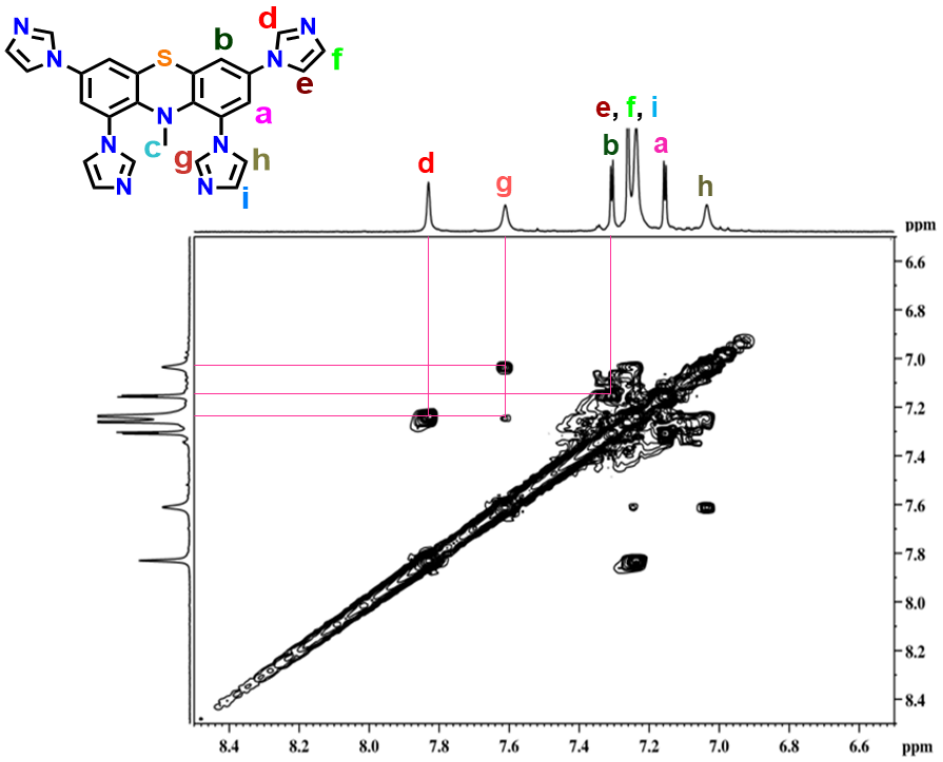

Fig. S7 ^{1}H 2D COSY NMR spectrum of ligand **L** recorded in $CDCl_3$.

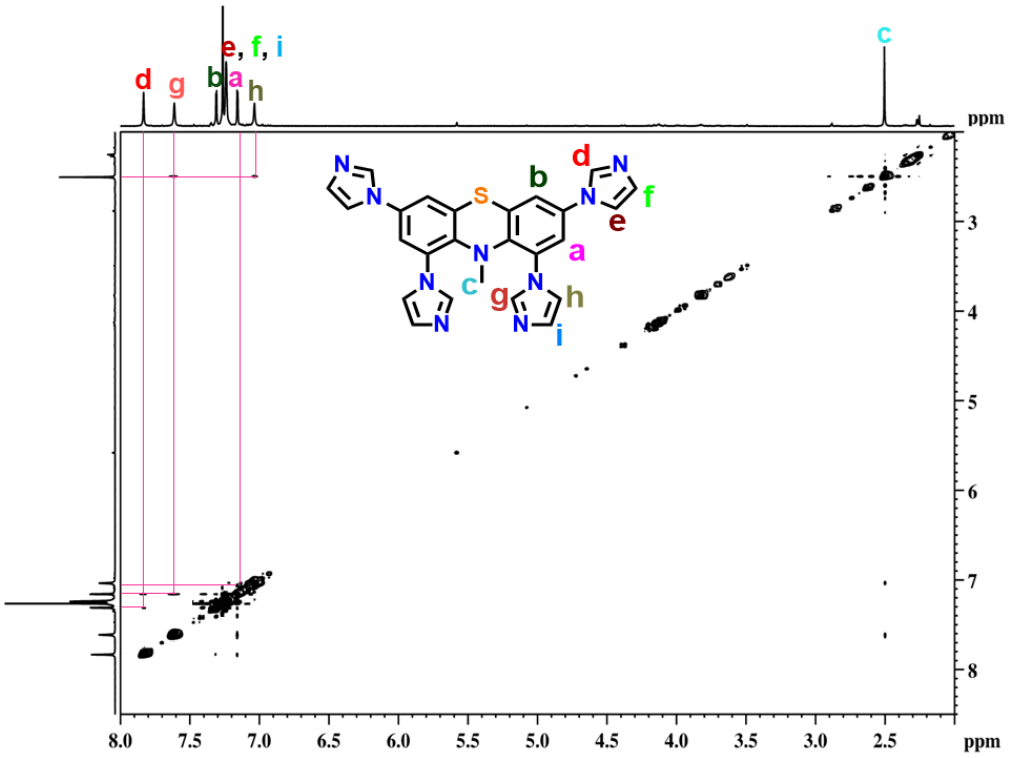

Fig. S8 ^{1}H 2D NOESY NMR spectrum of ligand **L** recorded in $CDCl_3$.

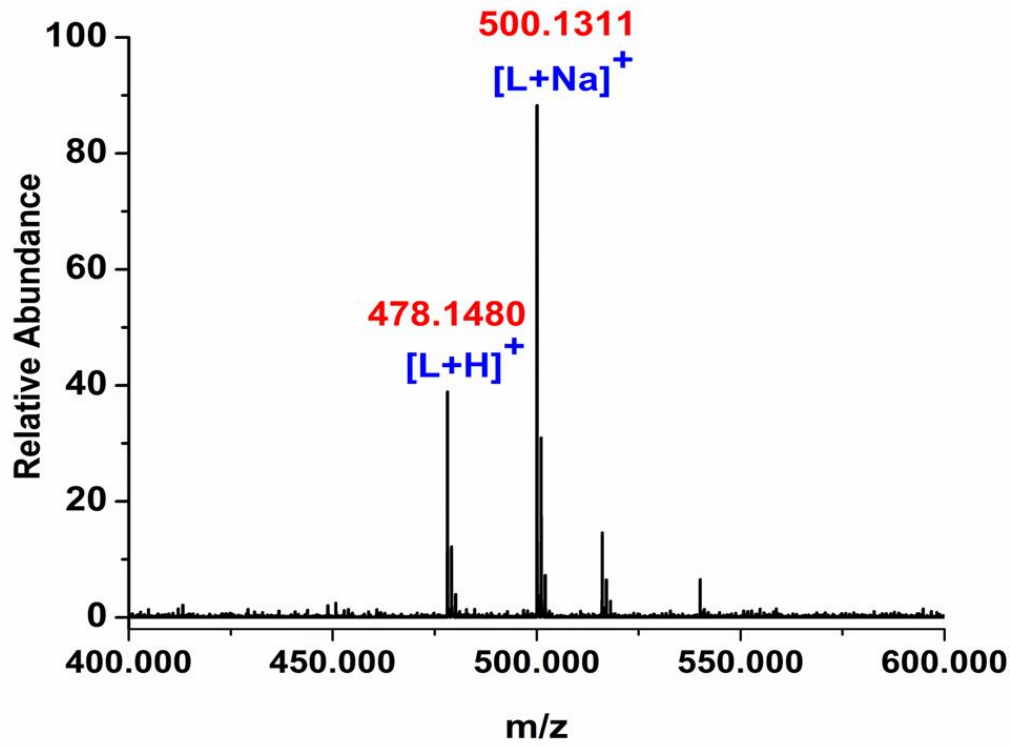

Fig. S9 ESI-MS spectrum of **L** recorded in MeOH.

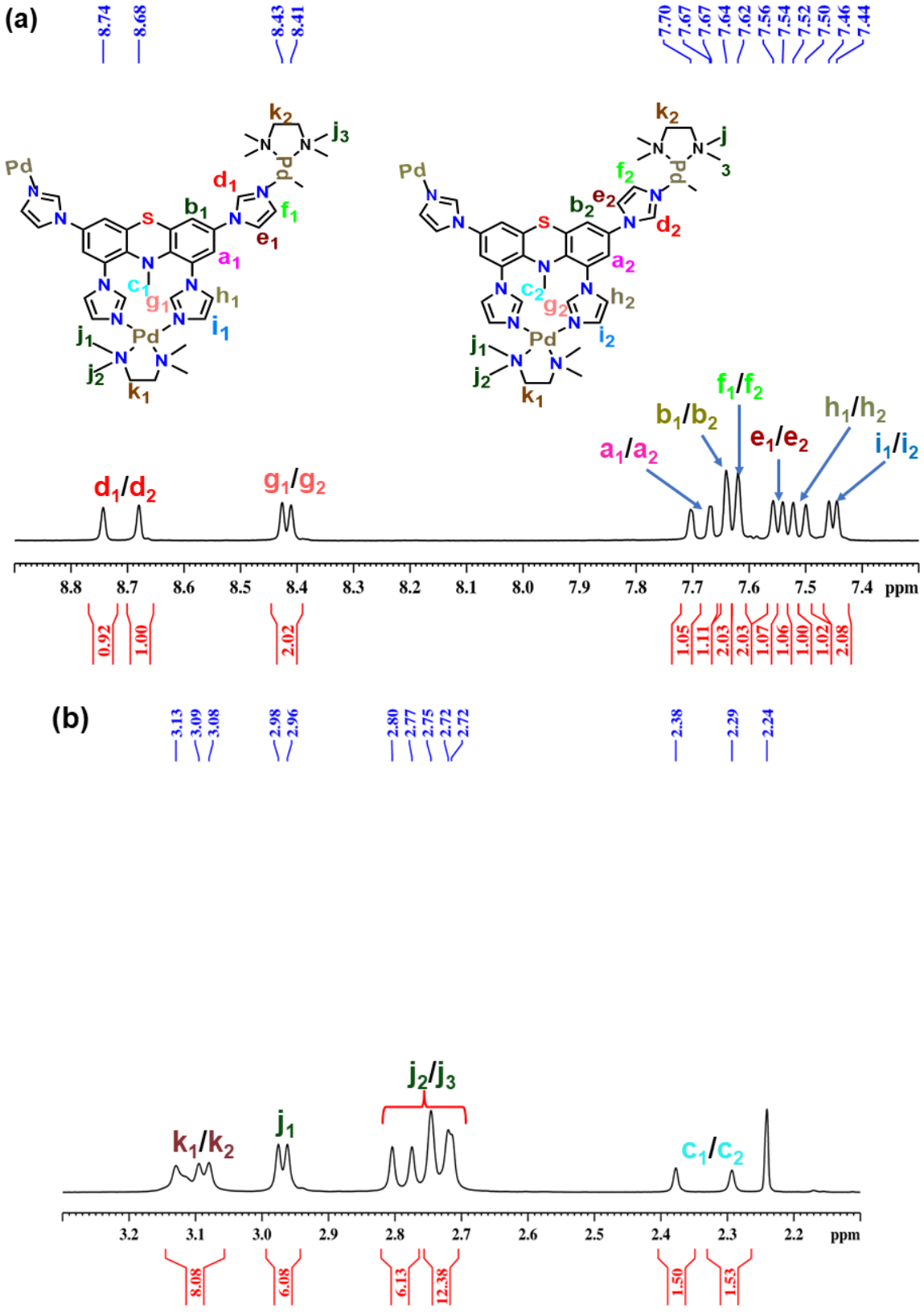

Fig. S10 Partial ^{1}H NMR spectra of aromatic protons (a) and aliphatic protons (b) of molecular tweezer **MT** recorded in D_2O.

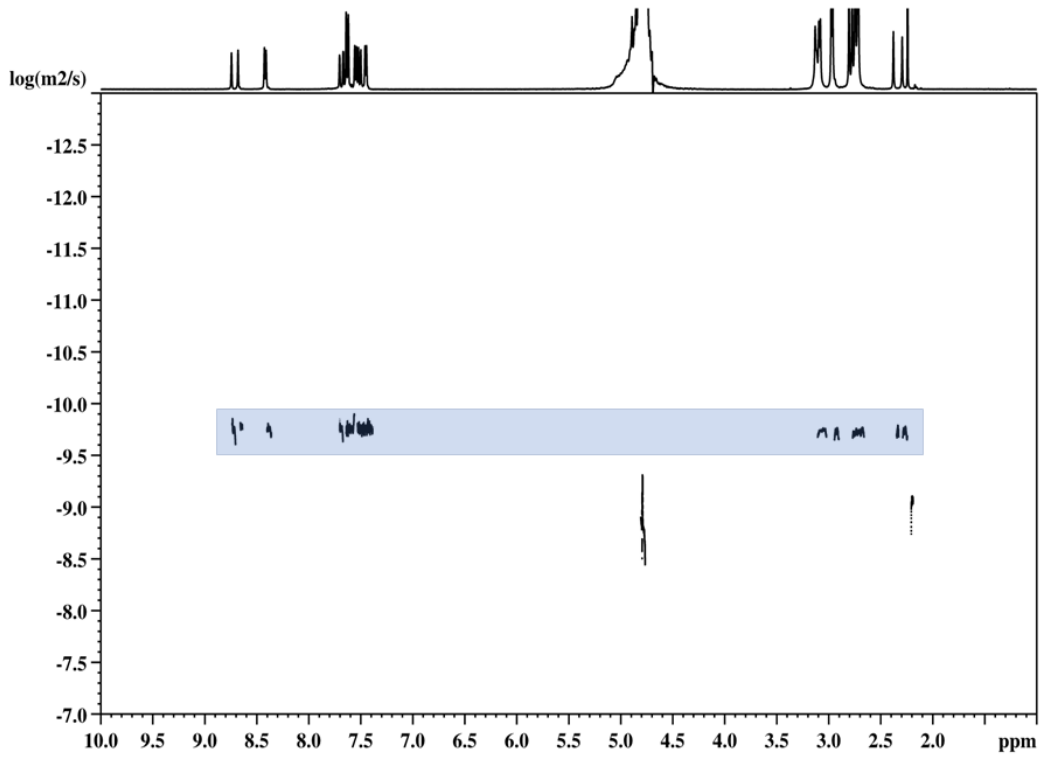

Fig. S11 ^{1}H 2D DOSY NMR spectrum of the molecular tweezer **MT** recorded in D_2O.

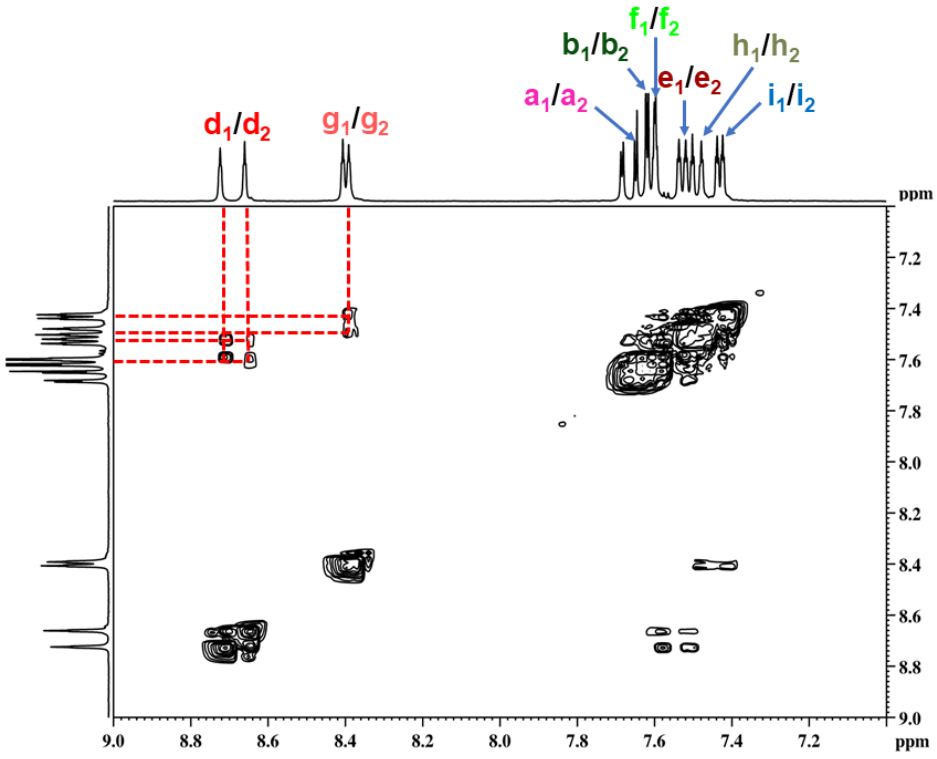

Fig. S12 ^{1}H 2D COSY NMR spectrum of the molecular tweezer **MT** recorded in D_2O.

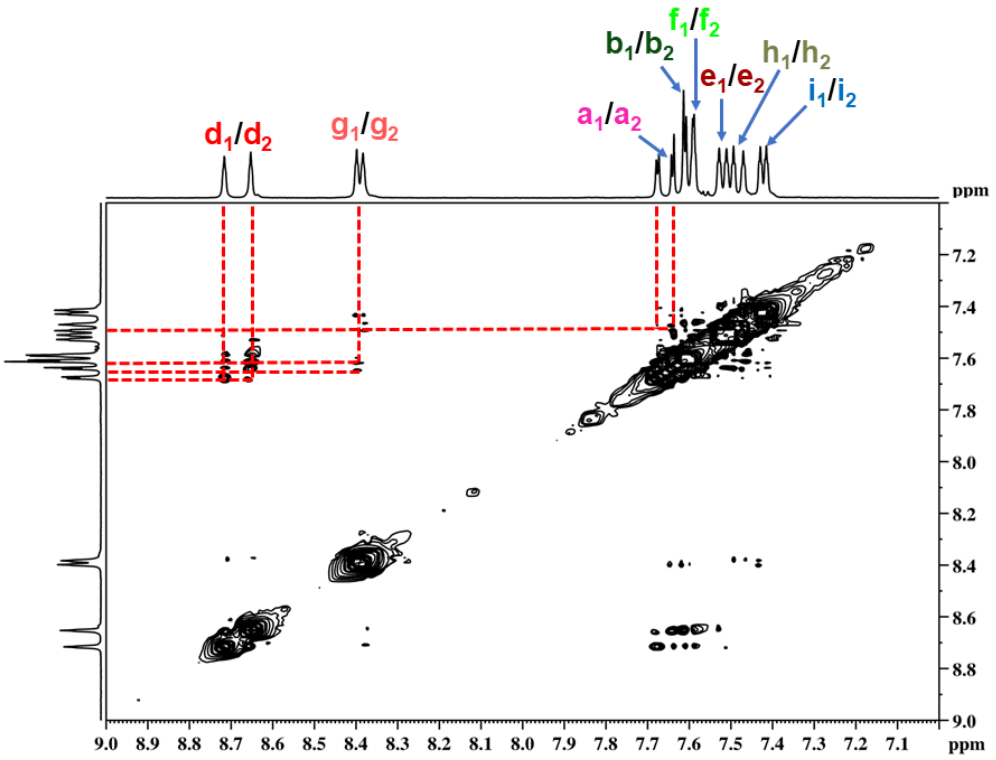

Fig. S13 ^{1}H 2D NOESY NMR spectrum of aromatic protons of the molecular tweezer **MT** recorded in D_2O.

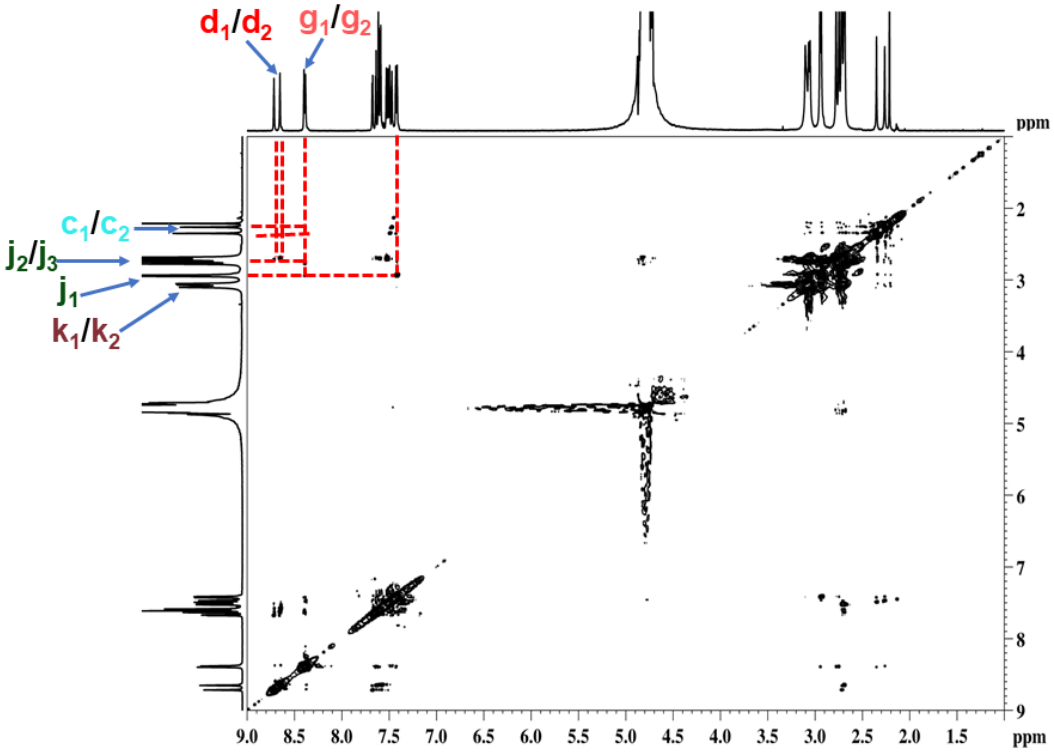

Fig. S14 ^{1}H 2D NOESY NMR spectrum (showing NOE correlation between the protons in the aliphatic region) of the molecular tweezer **MT** recorded in D_2O.

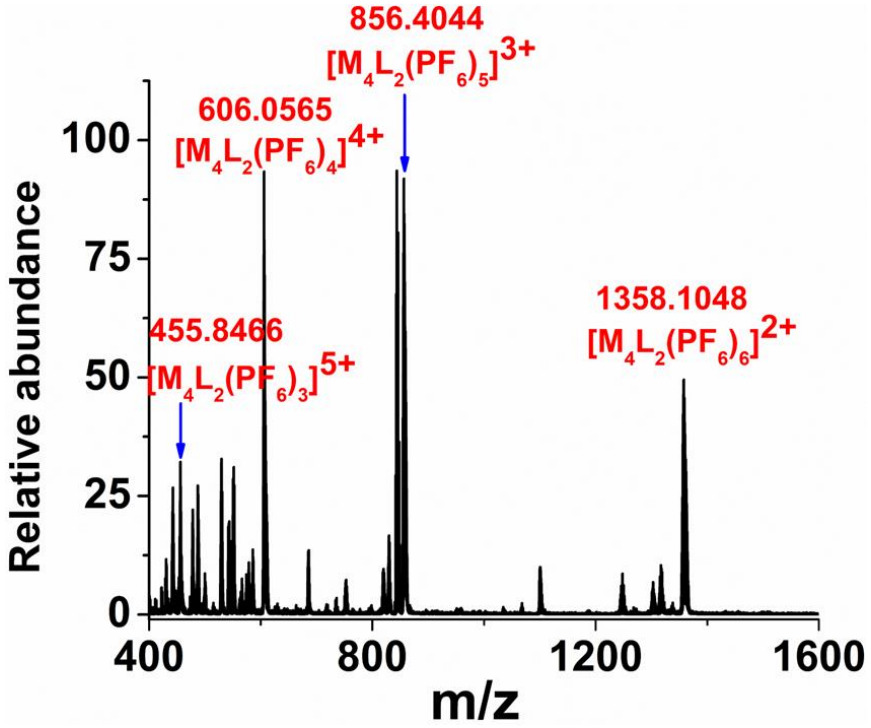

Fig. S15 ESI-MS full spectrum of the molecular tweezer **MT** recorded in CH_3CN.

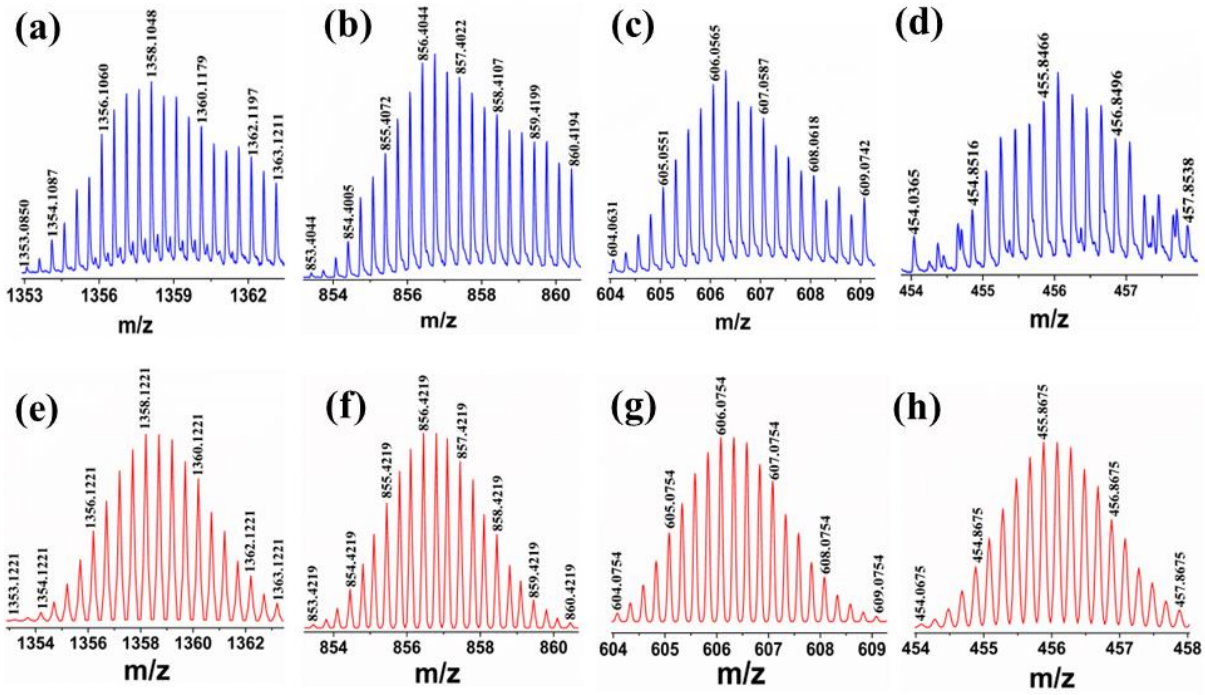

Fig. S16 Experimental (blue) isotopic distribution patterns of the mass-peaks corresponding to $[M_4L_2(PF_6)_6]^{2+}$ (a), $[M_4L_2(PF_6)_5]^{3+}$ (b), $[M_4L_2(PF_6)_4]^{4+}$ (c) and $[M_4L_2(PF_6)_3]^{5+}$ (d). Calculated (red) isotopic distribution patterns of the peaks corresponding to $[M_4L_2(PF_6)_6]^{2+}$ (e), $[M_4L_2(PF_6)_5]^{3+}$ (f), $[M_4L_2(PF_6)_4]^{4+}$ (g) and $[M_4L_2(PF_6)_3]^{5+}$ (h).

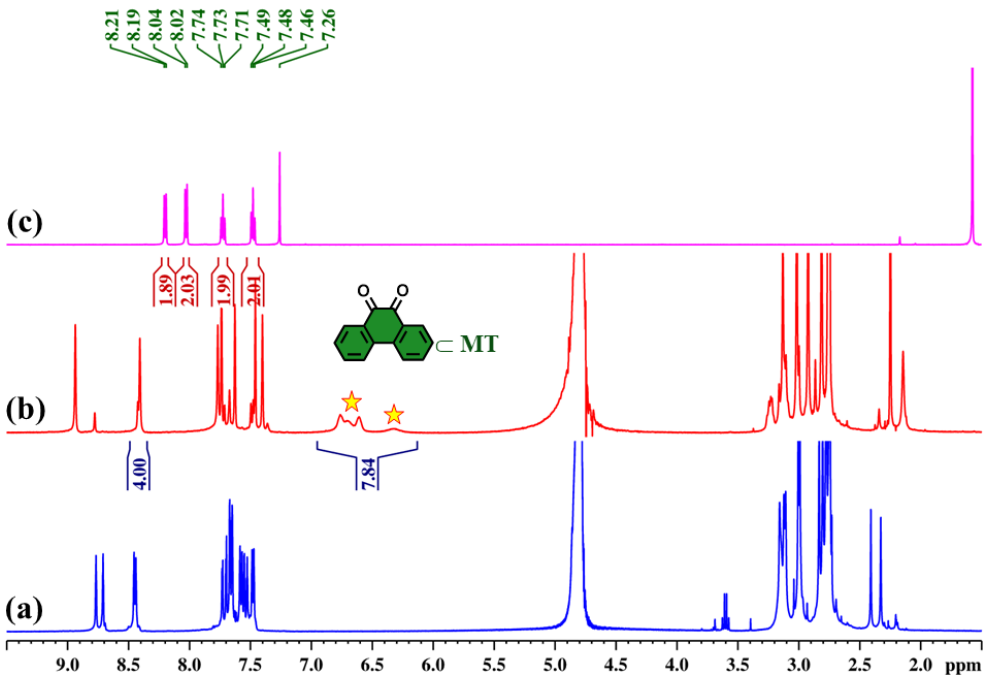

Fig. S17 Partial ^{1}H NMR spectrum of (a) MT, (b) PQ ⊂**MT** (in D_2O) and (c) PQ in $CDCl_3$ (500 MHz, 298 K).

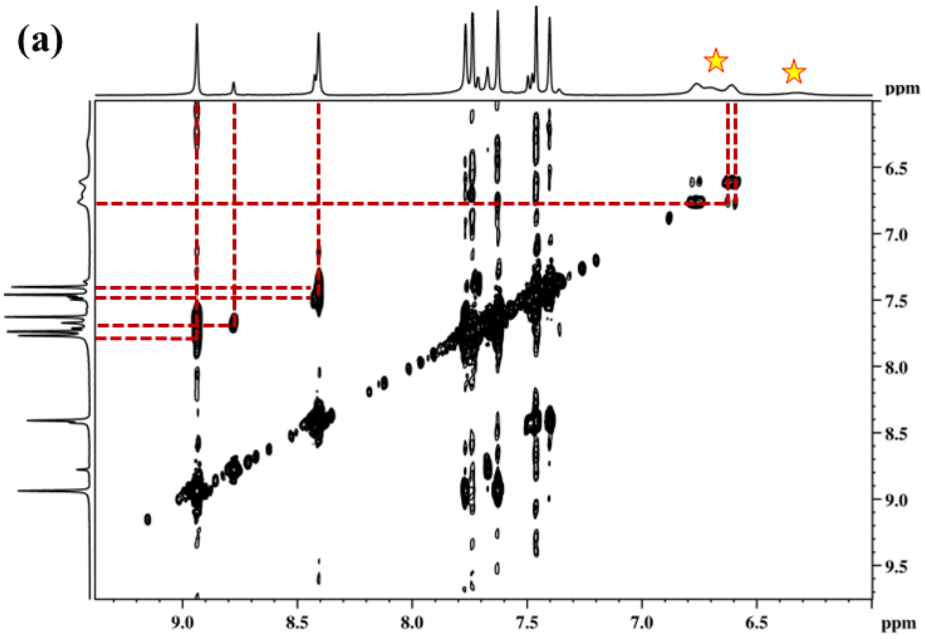

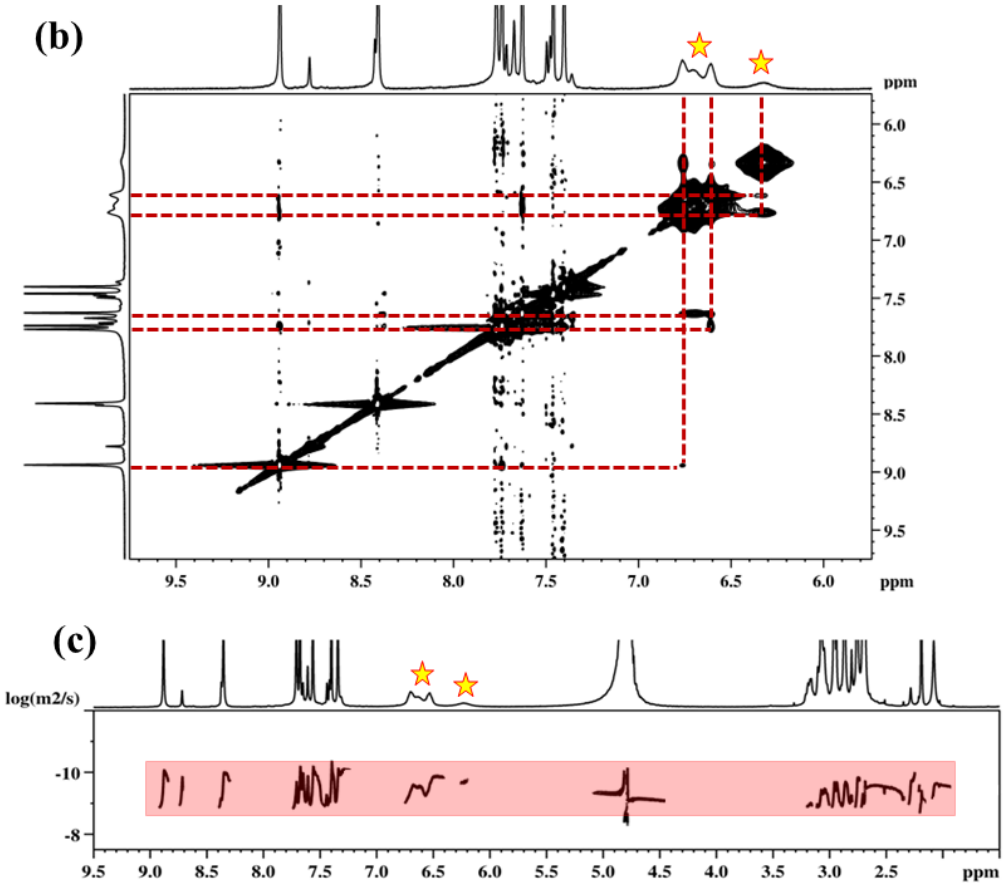

Fig. S18 Partial (a) ^{1}H-^{1}H COSY NMR spectrum, (b) ^{1}H-^{1}H NOESY NMR spectrum, and (c) ^{1}H 2D DOSY NMR spectrum of **PQ⊂MT** in D_2O (500 MHz, 298 K). Peaks of encapsulated guest are shown by yellow stars.

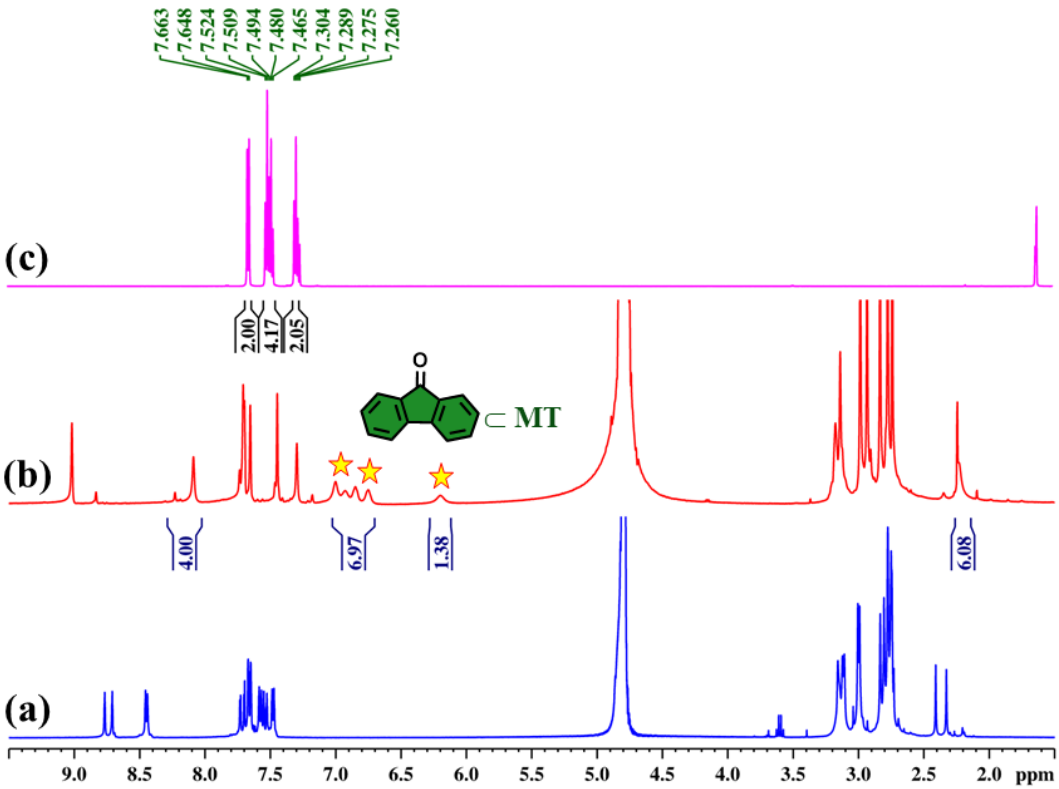

Fig. S19 Partial ^{1}H NMR spectrum of (a) MT, (b) **9-FN⊂MT** (in D_2O) and (c) **9-FN** in $CDCl_3$ (500 MHz, 298 K).

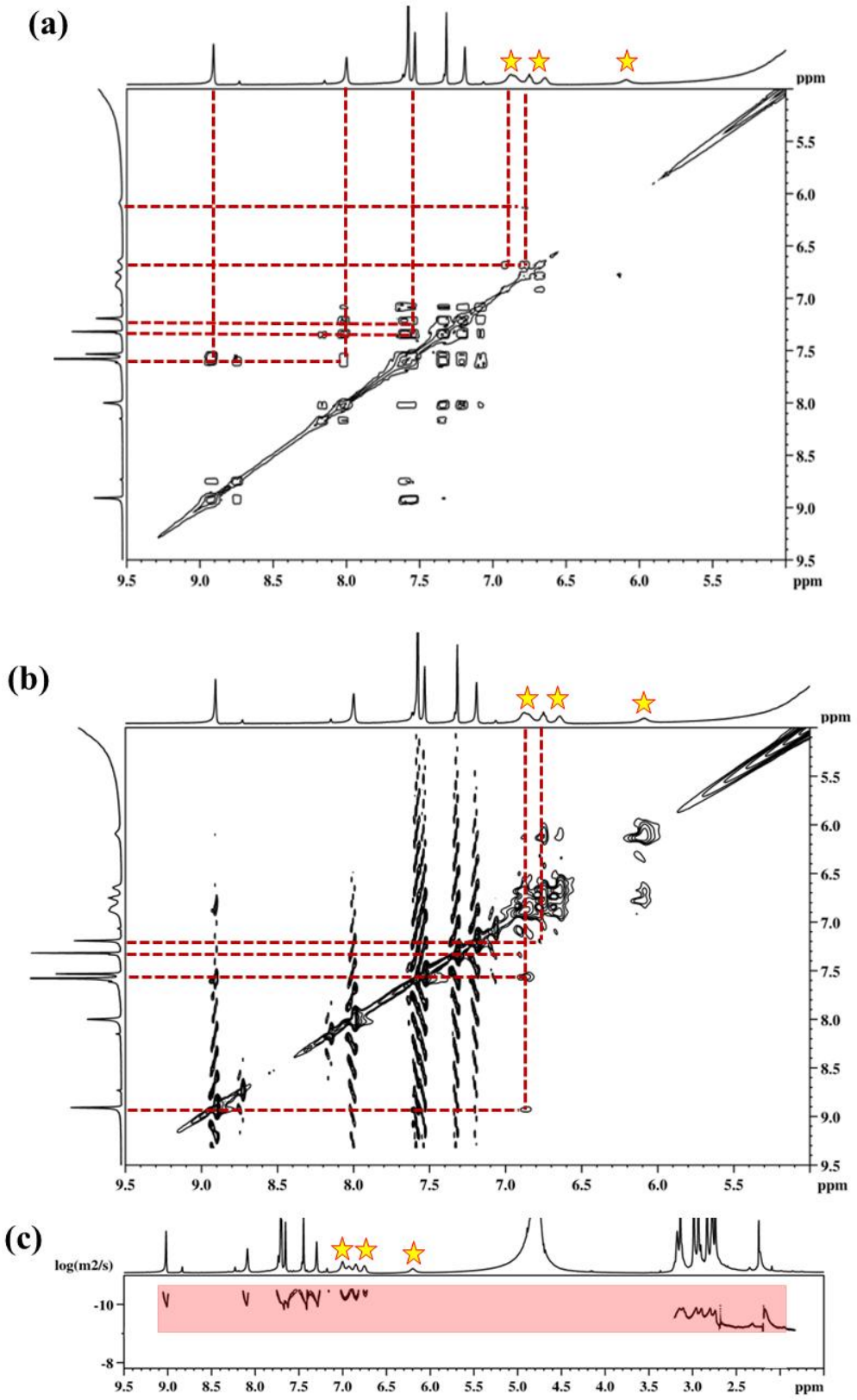

Fig. S20 Partial (a) ^{1}H-^{1}H COSY NMR spectrum, (b) ^{1}H-^{1}H NOESY NMR spectrum, and (c) ^{1}H 2D DOSY NMR spectrum of **9-FNQ⊂MT** in D_2O (500 MHz, 298 K). Peaks of encapsulated guest are shown by yellow stars.

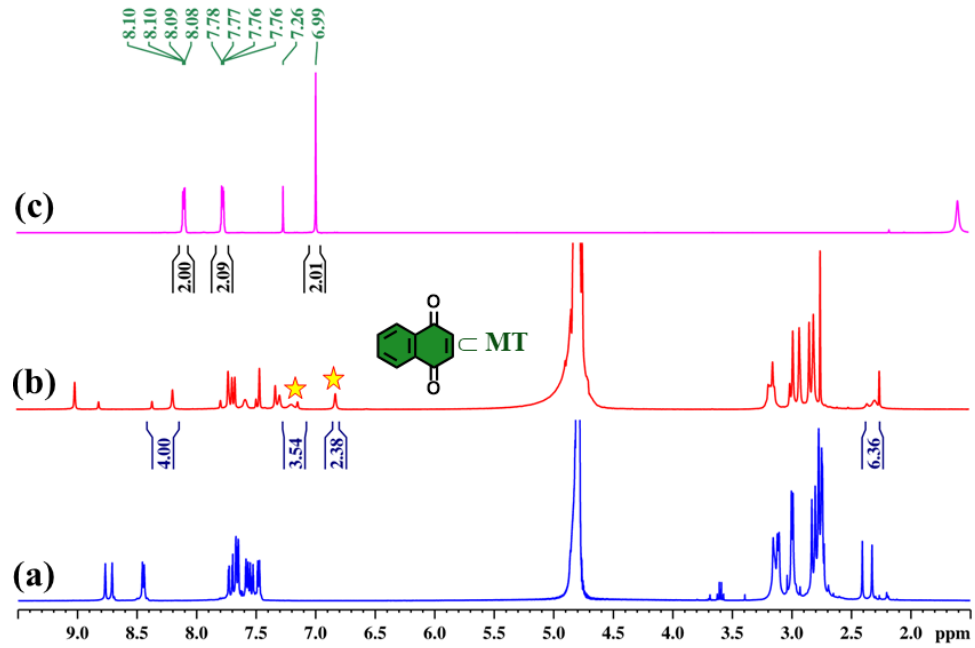

Fig. S21 Partial ^{1}H NMR spectrum of (a) **MT**, (b) **NQ⊂MT** (in D_2O) and (c) **NQ** in $CDCl_3$ (500 MHz, 298 K).

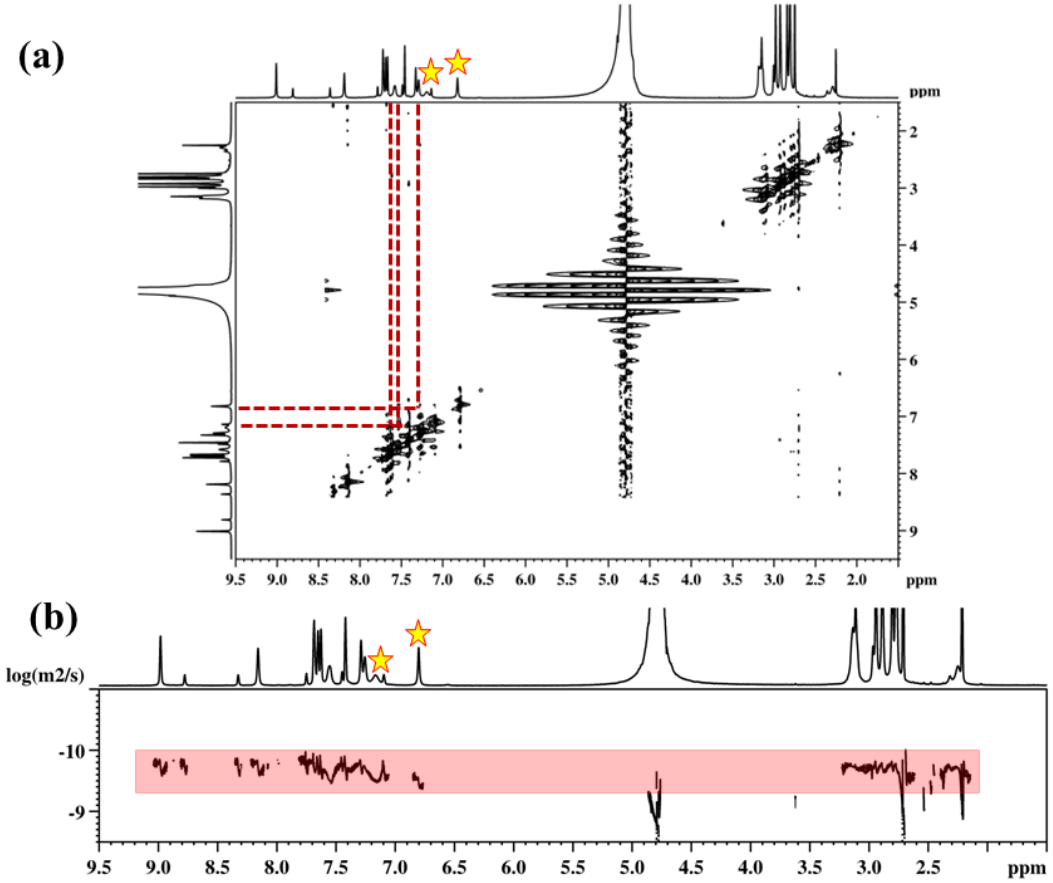

Fig. S22 Partial (a) ^{1}H-^{1}H NOESY NMR spectrum, and (b) ^{1}H 2D DOSY NMR spectrum of NQ⊂**MT** in D_2O (500 MHz, 298 K). Encapsulated guest peaks are shown by yellow stars.

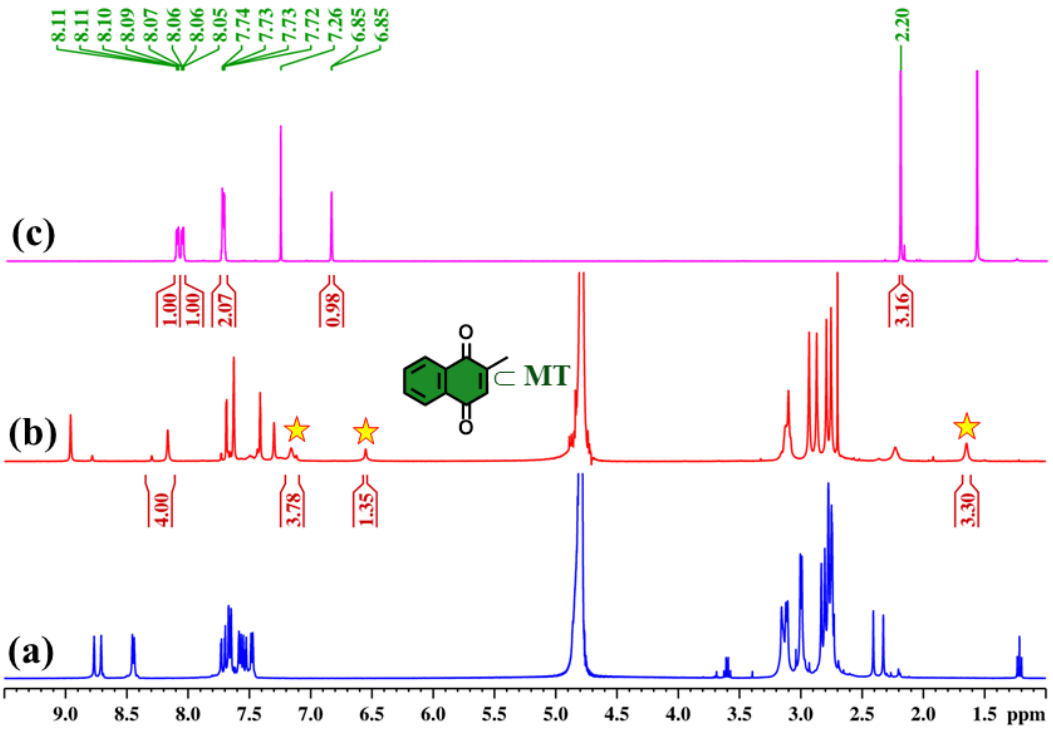

Fig. S23 Partial ^{1}H NMR spectrum of (a) **MT**, (b) **2-MeNQ ⊂ MT** (in D_2O) and (c) **2-MeNQ** in $CDCl_3$ (500 MHz, 298 K).

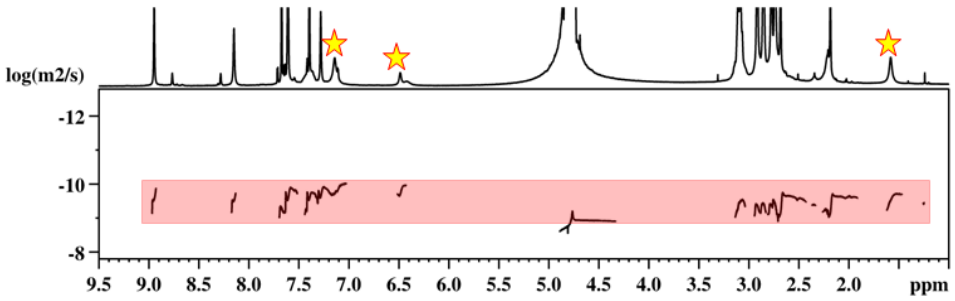

Fig. S24 ^{1}H 2D DOSY NMR spectrum of **2-MeNQ⊂MT** in D_2O (400 MHz, 298 K).

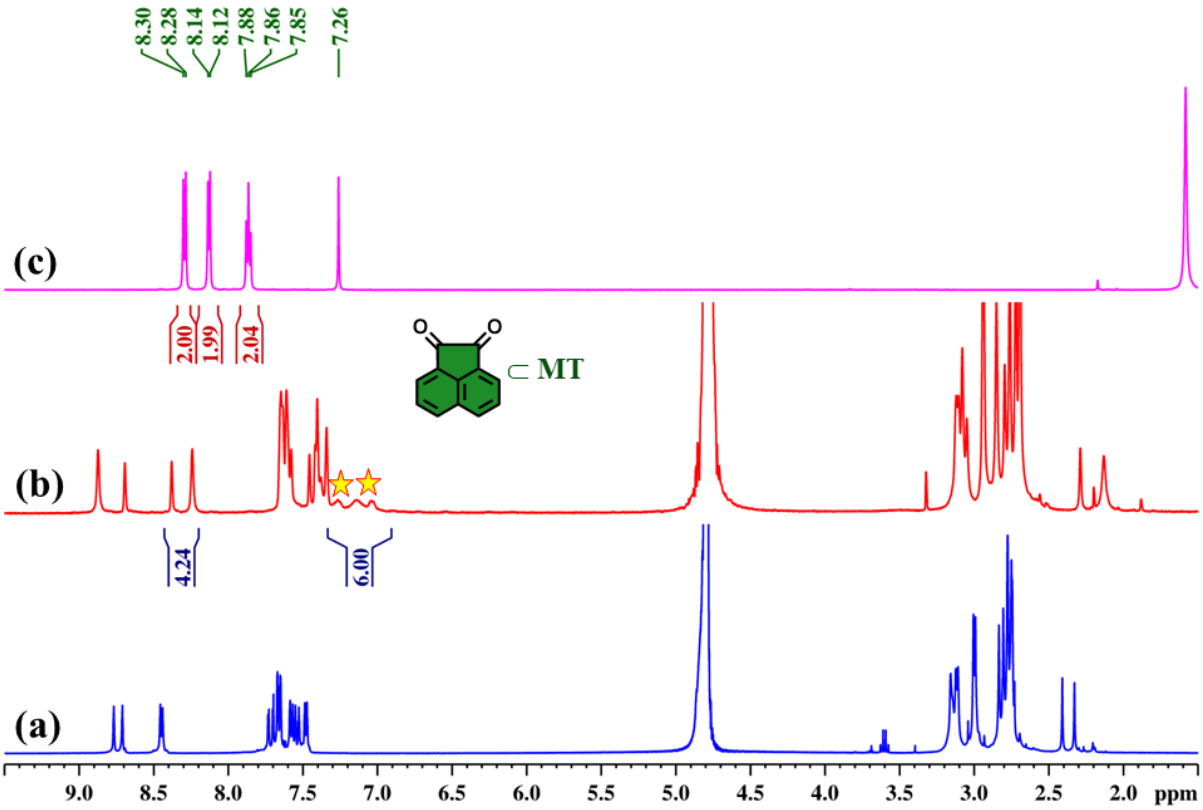

Fig. S25 Partial ^{1}H NMR spectrum of (a) MT, (b) **AceNQ⊂MT** (in D_2O) and (c) **AceNQ** in $CDCl_3$ (500 MHz, 298 K).

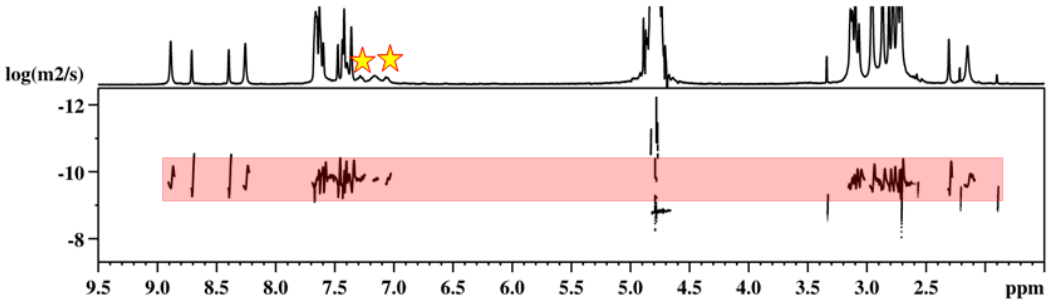

Fig. S26 ^{1}H 2D DOSY NMR spectrum of **AceNQ⊂MT** in D_2O (400 MHz, 298 K).

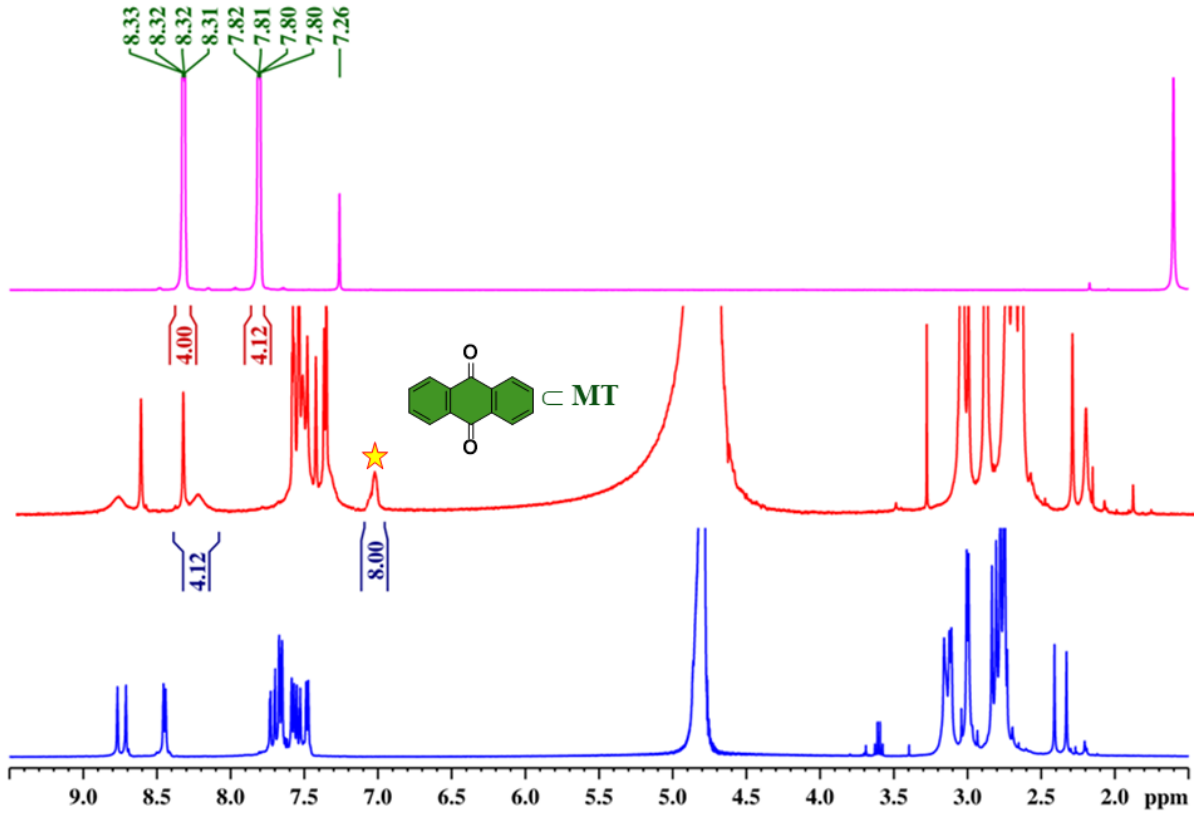

Fig. S27 Partial ^{1}H NMR spectrum of (a) MT, (b) **AQ⊂MT** (in D_2O) and (c) **AQ** in $CDCl_3$ (500 MHz, 298 K).

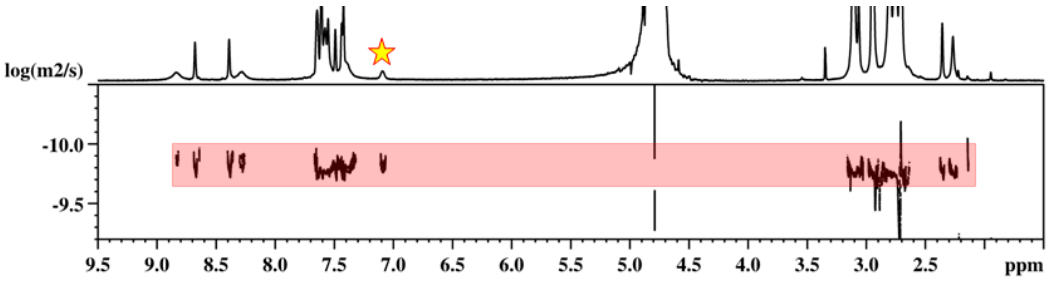

Fig. S28 ^{1}H 2D DOSY NMR spectrum of **AQ⊂MT** in D_2O (400 MHz, 298 K).

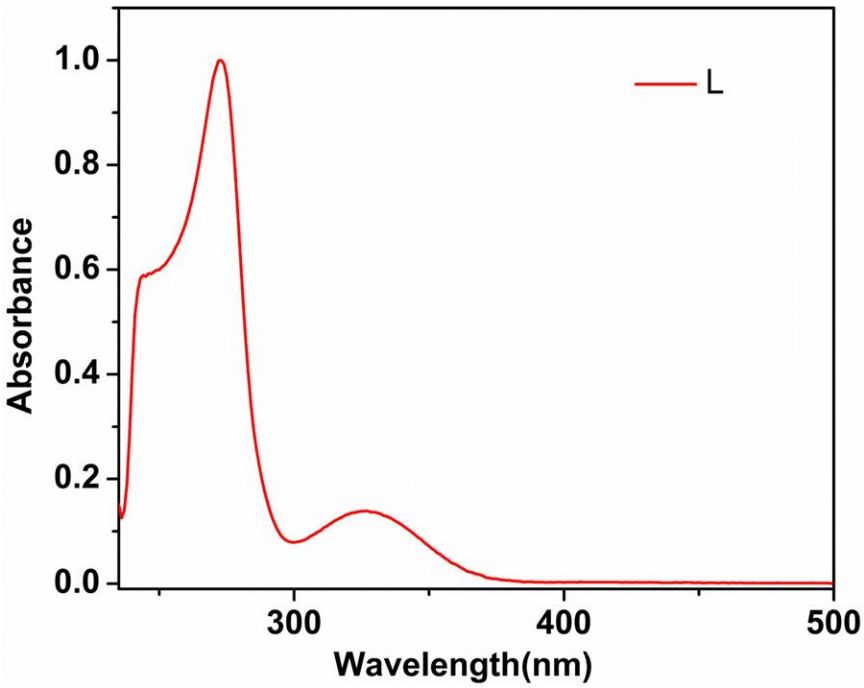

Fig. S29 Normalised absorption spectrum of **L** at room temperature in chloroform (10^{-5} M solution).

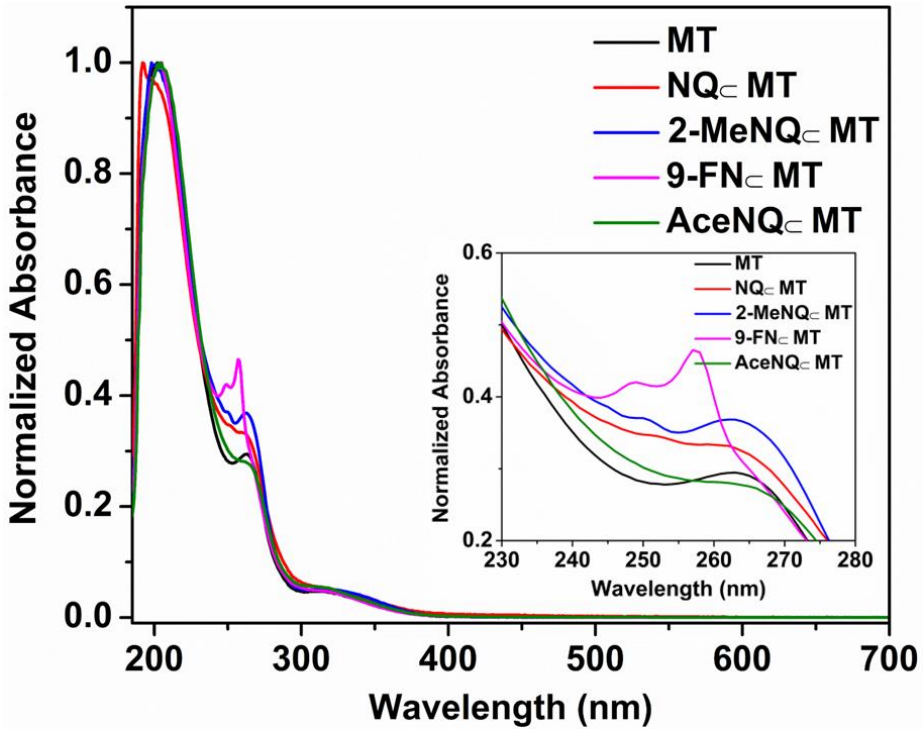

Fig. S30 Normalized absorption spectra of **MT**, **NQ⊂MT, 2-MeNQ⊂MT**, **9-FN⊂MT** and **AceNQ⊂MT** at room temperature in water (10^{-5} M solution). Inset picture shows enlarged absorption spectra.

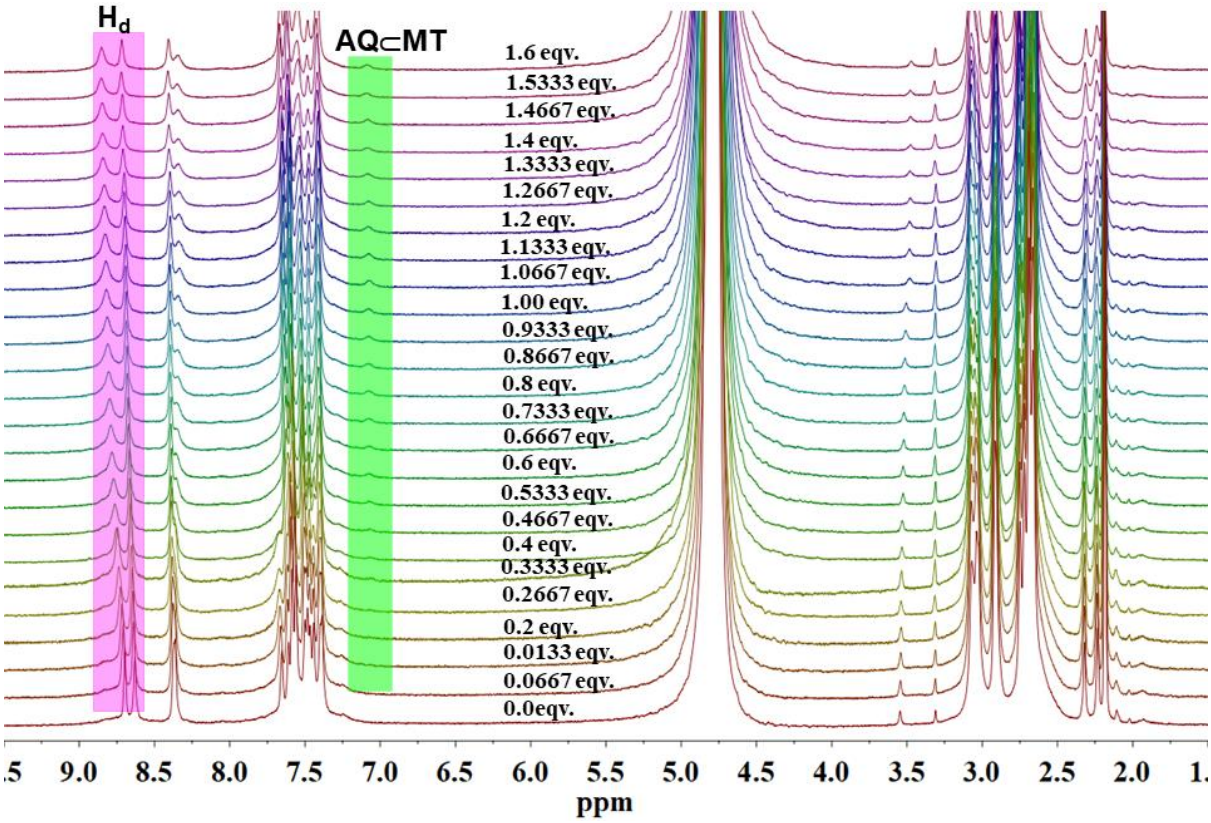

Fig. S31 ^{1}H NMR titration of MT (c = 5 mM) upon addition of 0–1.6 eqv. of AQ (AQ = anthraquinone, c = 0.04 M). Imidazole proton "H_d" is highlighted in the pink box. Peaks of encapsulated guest are highlighted in the green box.

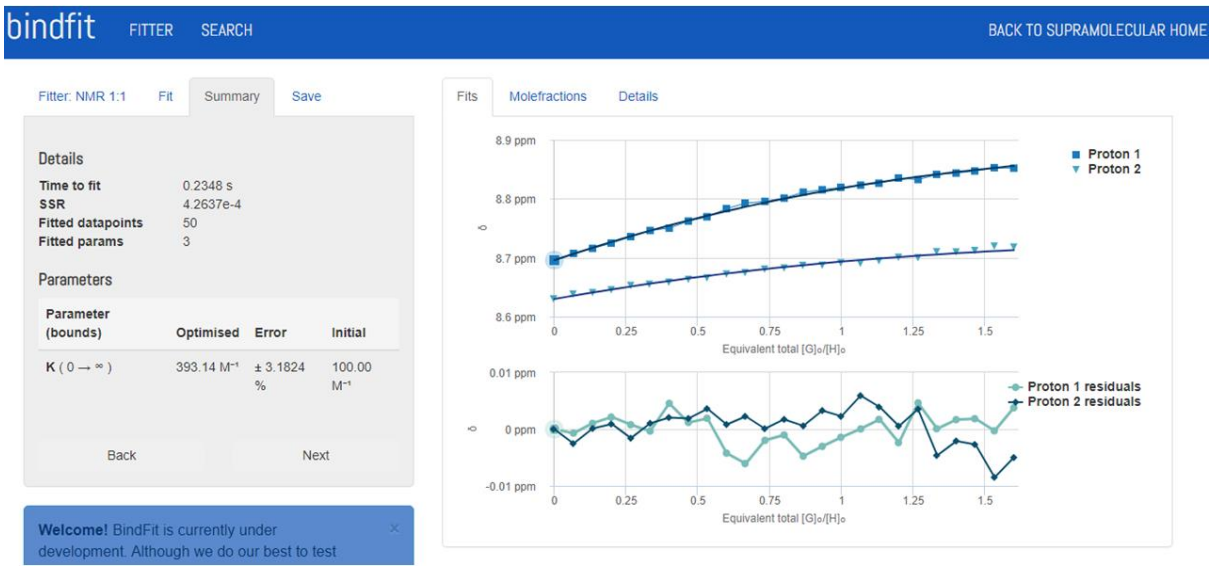

Fig. S32 Fitting of the titration data of **MT** with AQ in bindfit (http://supramolecular.org/) program using 1:1 (host:guest) binding model.

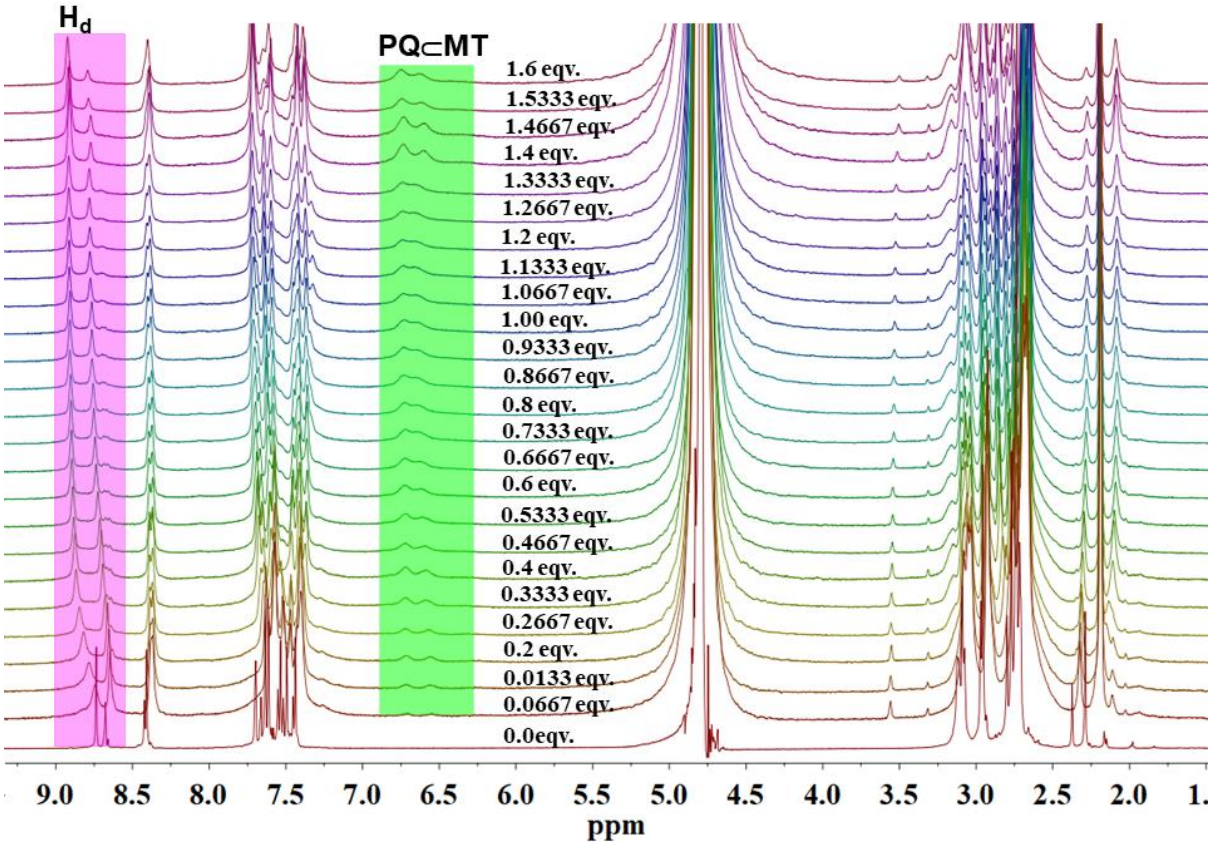

Fig. S33 ^{1}H NMR titration of **MT** (c = 5 mM) upon addition of 0–1.6 eqv. of PQ (PQ = phenanthrenequinone, c = 0.04 M). Imidazole proton "H_d" is highlighted in the pink box. Peaks of encapsulated guest are highlighted in the green box.

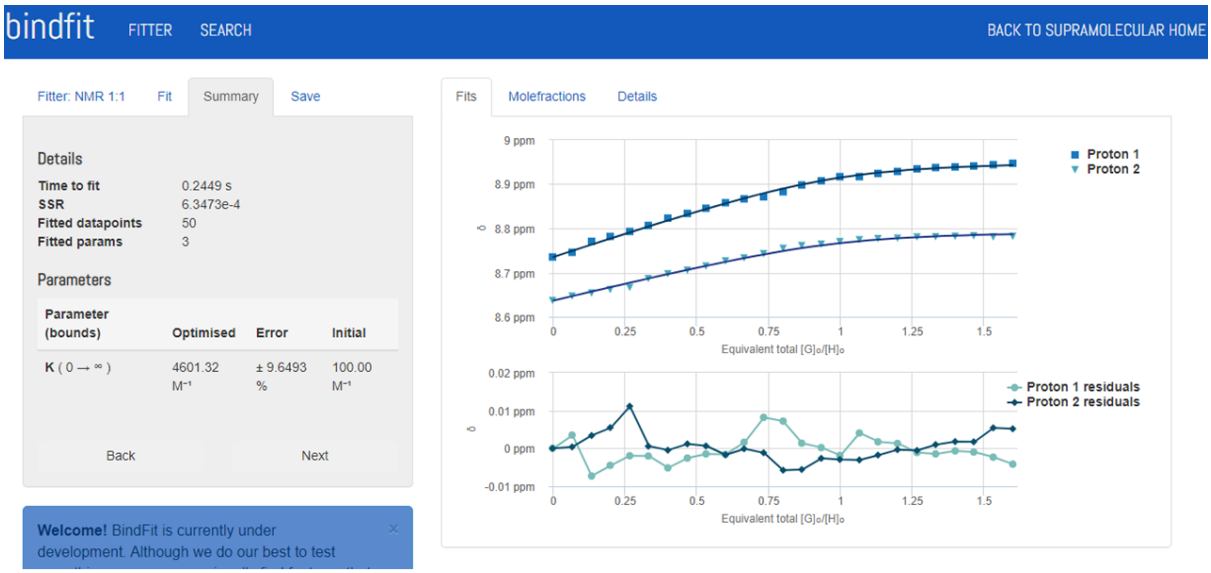

Fig. S34 Fitting of the titration data of **MT** with PQ in bindfit (http://supramolecular.org/) program using 1:1 (host: guest) binding model.

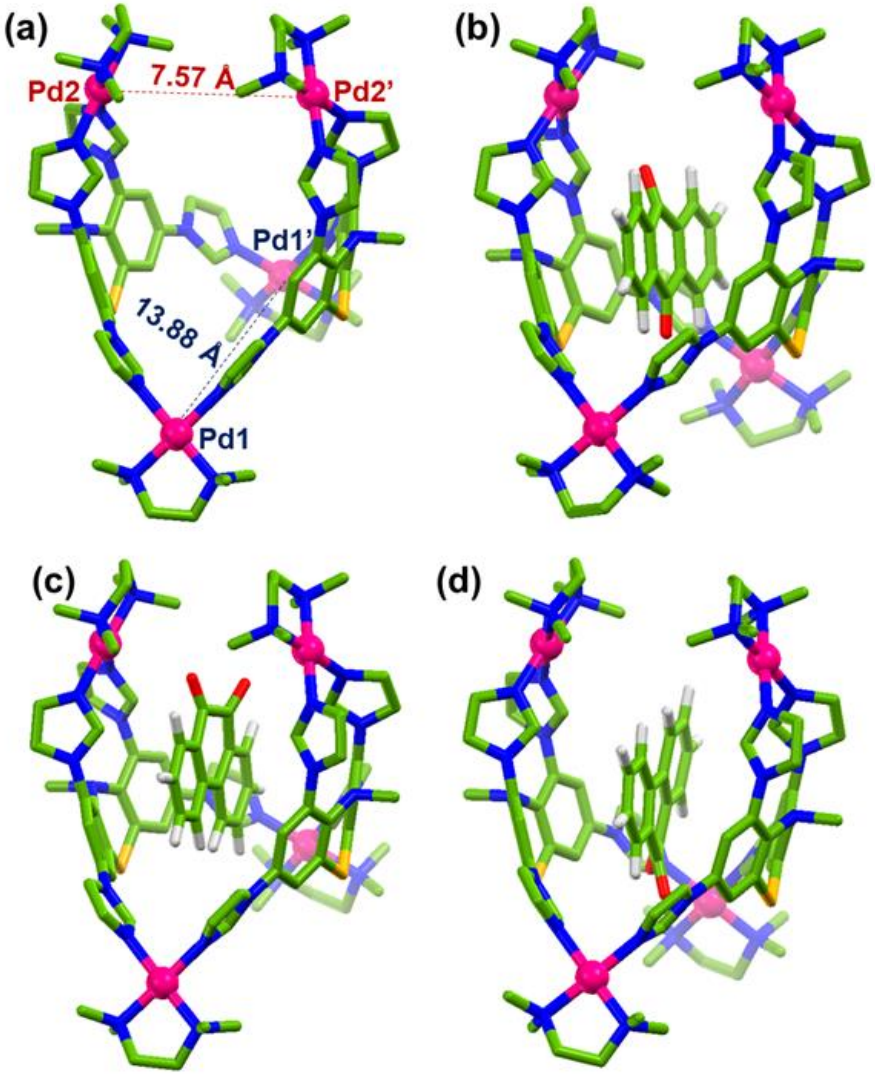

Fig. S35 Energy optimized structures of (a) free host (**MT**), (b) AQ⊂**MT**, (c) PQ⊂**MT** with diketone functional groups oriented upward (towards Pd2, Pd2'), and (d) PQ⊂**MT** where diketone functional groups oriented downward (towards Pd1, Pd1'). Single point energies calculations displayed more stability for PQ⊂**MT** with diketone functional groups oriented upward (towards Pd2, Pd2'). Colour codes: green = carbon, blue = nitrogen, yellow = sulphur, red = oxygen, grey = hydrogen and pink = palladium. H atoms of the host molecule are omitted for better clarity.

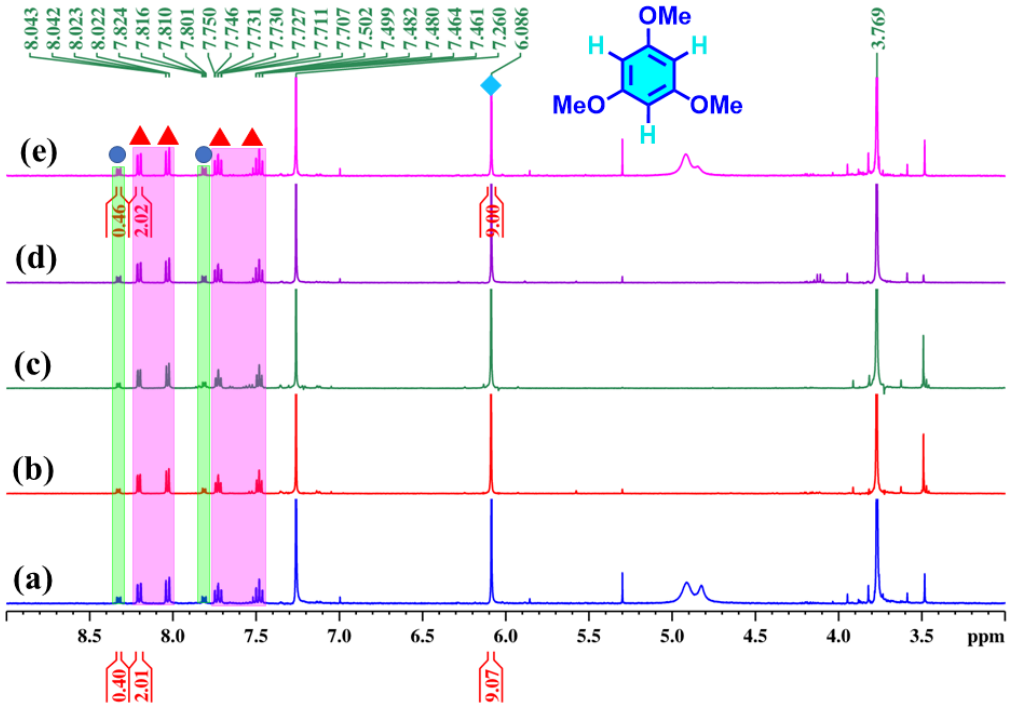

Fig. S36 Phenanthrenequinone extraction performance of **MT**: ^{1}H NMR spectra of $CDCl_3$ extract of the aqueous solution upon treating **MT** with 1:1: mixture of phenanthrenequinone, and anthraquinone. 3 eqv. of 1,3,5-trimethoxy benzene was used as an internal standard. After 1st cycle (a), 2nd cycle (b), 3rd cycle (c), 4th cycle (d), and 5th cycle (e), of extraction (400 MHz, 298 K). Peaks from phenanthrenequinone, anthraquinone and 1,3,5- trimethoxy benzene are shown by, red tringle, blue sphere, and cyan square respectively.

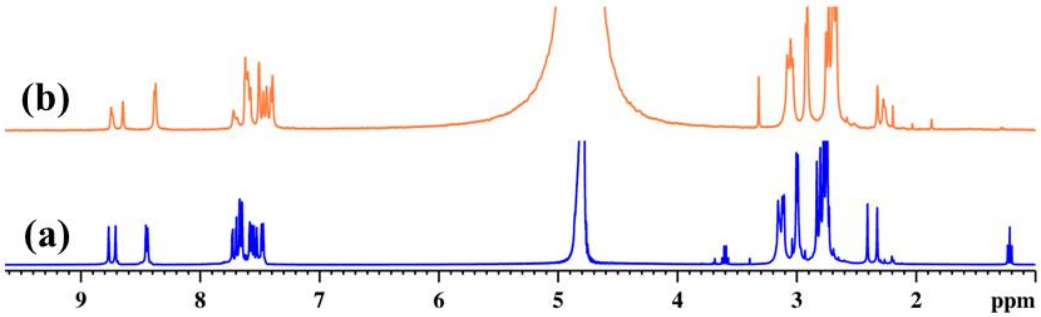

Fig. S37 Stability of **MT**: ^{1}H NMR spectra of **MT** (a)**,** and after five cycles of use of **MT** (b) for phenanthrenequinone extraction in D_2O (400 MHz, 298 K).

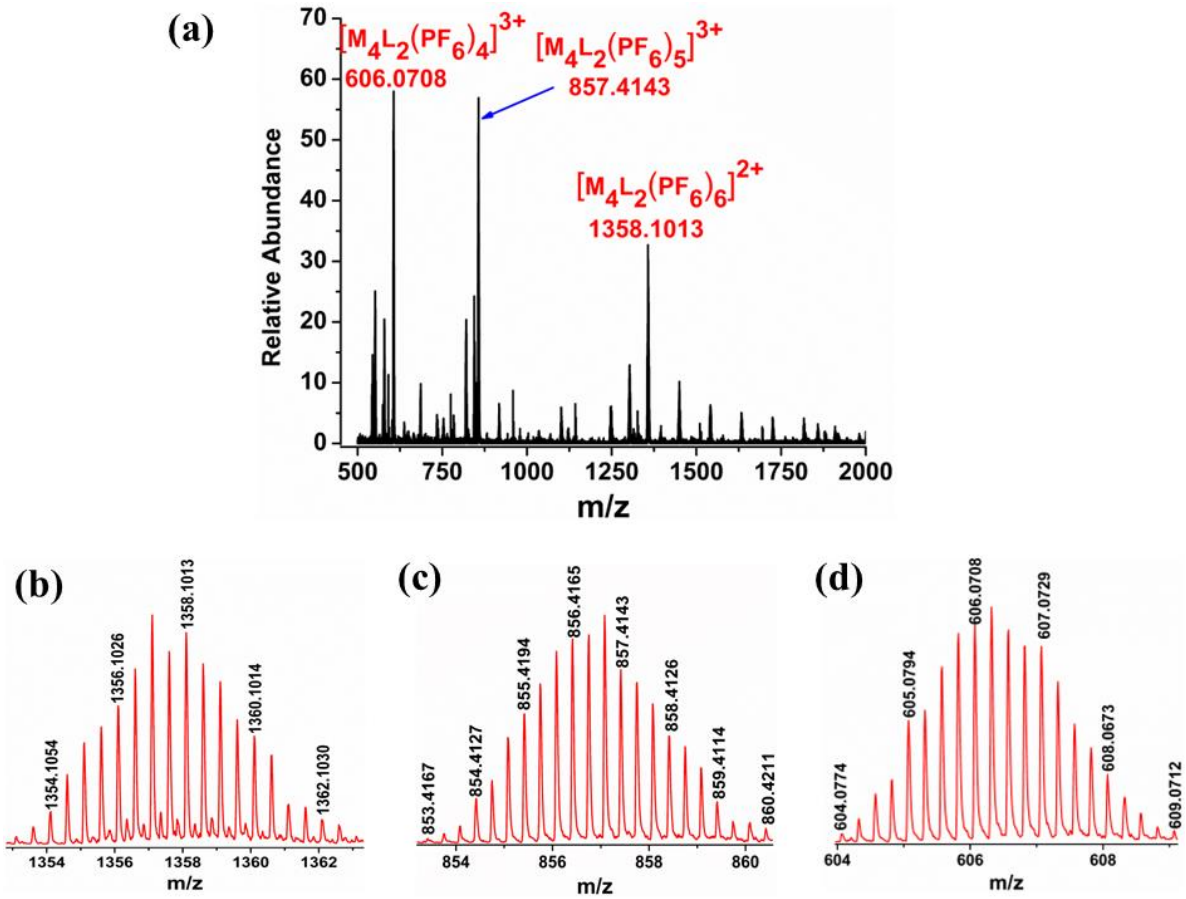

Fig. S38 ESI-MS of the recovered **MT**: Full ESI-MS spectrum in acetonitrile of the recovered M**T** after five cycles of phenanthrenequinone extraction (a); isotopic distribution patterns of the peaks correspond to fragments $[M_4L_2(PF_6)_6]^{2+}$ (b), $[M_4L_2(PF_6)_5]^{3+}$ (c), and $[M_4L_2(PF_6)_4]^{4+}$ (d).

References:

1. Y. Shindo, S. Nomura, Y. Saikawa, M. Nakata, K. Tanaka, K. Hanaya, T. Sugai, S. Higashibayashi, Synthesis and properties of hydrazine-embedded biphenothiazines and application of hydrazine-embedded heterocyclic compounds to fluorescence cell imaging. *Asian J. Org. Chem.,* 2018, **7**, 1797–1801.
2. W. Kabsch, XDS. *Acta Crystallogr. Sect. D Biol. Crystallogr.* 2010, **66**, 125–132.
3. M. C. Burla, R. Caliandro, B. Carrozzini, G. L. Cascarano, C. Cuocci, C. Giacovazzo, M. Mallamo, A. Mazzone, G. Polidori, Crystal structure determination and refinement via SIR2014. *J. Appl. Cryst*. 2015, **48**, 306–309.
4. G. M. Sheldrick, A short history of SHELX. *Acta Cryst.* 2008, **64**, 112–122.

5. A. L. Spek, PLATON, An integrated tool for the analysis of the results of a single crystal structure determination. *Acta Cryst*. 1990, **46**, c34.
6. M. J. Frisch, G. W. Trucks, H. B. Schlegel, G. E. Scuseria, M. A. Robb, J. R. Cheeseman, G. Scalmani, V. Barone, B. Mennucci, G. A. Petersson, H. Nakatsuji, M. Caricato, X. Li, H. P. Hratchian, A. F. Izmaylov, J. Bloino, G. Zheng, J. L. Sonnenberg, M. Hada, M. Ehara, K. Toyota, R. Fukuda, J. Hasegawa, M. Ishida, T. Nakajima, Y. Honda, O. Kitao, H. Nakai, T. Vreven, J. A. Jr. Montgomery, J. E. Peralta, F. Ogliaro, M. Bearpark, J. J. Heyd, E. Brothers, K. N. Kudin, V. N. Staroverov, R. Kobayashi, J. Normand, K. Raghavachari, A. Rendell, J. C. Burant, S. S. Iyengar, J. Tomasi, M. Cossi, N. Rega, J. M. Millam, M. Klene, J. E. Knox, J. B. Cross, V. Bakken, C. Adamo, J. Jaramillo, R. Gomperts, R. E. Stratmann, O. Yazyev, A. J. Austin, R. Cammi, C. Pomelli, J. W. Ochterski, R. L. Martin, K. Morokuma, V. G. Zakrzewski, G. A. Voth, P. Salvador, J. J. Dannenberg, S. Dapprich, A. D. Daniels, O. Farkas, J. B. Foresman, J. V. Ortiz, J. Cioslowski, D. J. Fox, Gaussian 16, Revision C. 01, *Gaussian. Inc.*, *Wallingford CT* 2019.